Journal Pre-proof

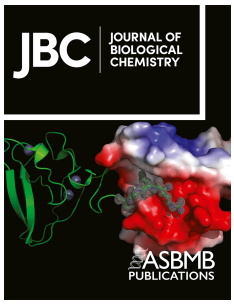

The dipeptide prolyl-hydroxyproline promotes cellular homeostasis and lamellipodia-driven motility via active β1-integrin in adult tendon cells

Kentaro Ide, Sanai Takahashi, Keiko Sakai, Yuki Taga, Tomonori Ueno, David Dickens, Rosalind Jenkins, Francesco Falciani, Takako Sasaki, Kazuhiro Ooi, Shuichi Kawashiri, Kazunori Mizuno, Shunji Hattori, Takao Sakai

PII: S0021-9258(21)00615-3

DOI: https://doi.org/10.1016/j.jbc.2021.100819

Reference: JBC 100819

To appear in: *Journal of Biological Chemistry*

Received Date: 22 February 2021

Revised Date: 8 May 2021

Accepted Date: 20 May 2021

Please cite this article as: Ide K, Takahashi S, Sakai K, Taga Y, Ueno T, Dickens D, Jenkins R, Falciani F, Sasaki T, Ooi K, Kawashiri S, Mizuno K, Hattori S, Sakai T, The dipeptide prolyl-hydroxyproline promotes cellular homeostasis and lamellipodia-driven motility via active β1-integrin in adult tendon cells, *Journal of Biological Chemistry* (2021), doi: https://doi.org/10.1016/j.jbc.2021.100819.

The dipeptide prolyl-hydroxyproline promotes cellular homeostasis and lamellipodia-driven motility via active β1-integrin in adult tendon cells

Kentaro Ide[1#]*, Sanai Takahashi[1#], Keiko Sakai[1], Yuki Taga[2], Tomonori Ueno[2], David Dickens[1], Rosalind Jenkins[1], Francesco Falciani[3], Takako Sasaki[4], Kazuhiro Ooi[5], Shuichi Kawashiri[5], Kazunori Mizuno[2], Shunji Hattori[2], and Takao Sakai[1]

[1]MRC Centre for Drug Safety Science, Department of Pharmacology and Therapeutics, Institute of Systems, Molecular and Integrative Biology, University of Liverpool, Liverpool L69 3GE, UK;
[2]Nippi Research Institute of Biomatrix, Toride, Ibaraki 302-0017, Japan;
[3]Department of Biochemistry and Systems Biology, Institute of Systems, Molecular and Integrative Biology, University of Liverpool, Liverpool L69 3BX, UK;
[4]Department of Biochemistry, Faculty of Medicine, Oita University, Oita, 879-5593, Japan;
[5]Department of Oral and Maxillofacial Surgery, Kanazawa University Graduate School of Medical Science, Kanazawa, Ishikawa 920-8640, Japan

Running title: Effect of Pro-Hyp on tendon cells

Footnotes

[#], These authors contributed equally to this study.
*, Present address: Department of Oral and Maxillofacial Surgery, Kanazawa University Graduate School of Medical Science, Kanazawa, Ishikawa 920-8640, Japan

Key Words: Collagen-derived peptide; Prolyl-hydroxyproline; Adult tendon cells; Extracellular matrix; Scleraxis; Cell motility; Extracellular signal-regulated kinase.

Correspondence: Takao Sakai, M.D., Ph.D., MRC Centre for Drug Safety Science, Department of Pharmacology and Therapeutics, Institute of Systems, Molecular and Integrative Biology, University of Liverpool, Sherrington Building, Ashton Street, Liverpool L69 3GE, United Kingdom.
TEL: 0151-795-2704; FAX: 0151-794-5540; Email: sakait@liverpool.ac.uk

Abbreviations**:** DAVID, Database for Annotation, Visualization and Integrated Discovery; ECM, extracellular matrix; ERK, extracellular signal-regulated kinase; FBS, fetal bovine serum; FGF, fibroblast growth factor; GFP, green fluorescent protein; Hyp, hydroxyproline; IPA, ingenuity pathway analysis; LC-MS, liquid chromatography–mass spectrometry; MAPK, mitogen-activated protein kinase; MEK, mitogen-activated protein kinase kinase; MKX, mohawk; Pro, proline; PDGF, platelet-derived growth factor; SCX, scleraxis; SOX 9, SRY-box 9; TGF-β, transforming growth factor-beta; TNMD, tenomodulin.

Grant Support: This work was supported in part by the Knowledge Exchange Funding Scheme, University of Liverpool, UK, and Nippi, Inc., Japan (to T. Sakai).

Acknowledgments: We thank Drs Tom Waring, Jennifer Adcott, and Marco Marcello, Centre for Cell Imaging, University of Liverpool, for expert technical assistance in time-lapse microscopic analysis, and Dr Larry Fisher, National Institute of health, USA, and Dr. Donald Gullberg, Institute of BioMedicine, University of Bergen, Norway, for antibodies. We thank Mr. Masashi Kusubata at Nippi Inc. for valuable comments, and Dr. Gerald E. Smyth for editorial assistance.

Author contributions: Takao Sakai conceived the ideas, designed the experiments, and supervised the project. Kentaro Ide, Sanai Takahashi, Keiko Sakai, Yuki Taga, and Tomonori Ueno performed experiments. Rosalind Jenkins and Francesco Falciani performed proteomics analysis. Kentaro Ide, Keiko Sakai, Sanai Takahashi, Yuki Taga, Tomonori Ueno, Kazunori Mizuno, Shunji Hattori, David Dickens, Takako Sasaki, Kazuhiro Ooi, Shuichi Kawashiri, and Takao Sakai analyzed the data and discussed the interpretation of experimental results. Kentaro Ide and Takao Sakai drafted the manuscript, and Takao Sakai edited it.

Conflict of interest: No conflicts of interest, financial or otherwise, are declared by the authors.

Abstract

Collagen-derived hydroxyproline (Hyp)-containing peptides have a variety of biological effects on cells. These bioactive collagen peptides are locally generated by the degradation of endogenous collagen in response to injury. However, no comprehensive study has yet explored the functional links between Hyp-containing peptides and cellular behavior. Here, we show that the dipeptide prolyl-4-hydroxyproline (Pro-Hyp) exhibits pronounced effects on mouse tendon cells. Pro-Hyp promotes differentiation/maturation of tendon cells with modulation of lineage-specific factors and induces significant chemotactic activity *in vitro*. In addition, Pro-Hyp has profound effects on cell proliferation, with significantly upregulated ERK-phosphorylation and extracellular matrix production and increased type I collagen network organization. Using proteomics, we have predicted molecular transport, cellular assembly and organization, and cellular movement as potential linked-network pathways that could be altered in response to Pro-Hyp. Mechanistically, cells treated with Pro-Hyp demonstrate increased directional persistence, and significantly increased directed motility and migration velocity. They are accompanied by elongated lamellipodial protrusions with increased levels of active β1-integrin-containing focal contacts, as well as reorganization of thicker peripheral F-actin fibrils. Pro-Hyp-mediated chemotactic activity is significantly reduced ($P < 0.001$) in cells treated with the MEK1/2 inhibitor PD98059 or the α5β1-integrin antagonist ATN-161. Furthermore, ATN-161 significantly inhibits uptake of Pro-Hyp into adult tenocytes. Thus, our findings document the molecular basis of the functional benefits of the Pro-Hyp dipeptide in cellular behavior. These dynamic properties of collagen-derived Pro-Hyp dipeptide could lead the way to its application in translational medicine.

Introduction

Collagen is the most abundant extracellular matrix (ECM) protein in tissue/organ stroma and significantly contributes to tissue/organ integrity (1). Collagen contains at least one domain of repeated sequences of glycine (Gly)-X-Y, where X and Y are most frequently proline (Pro) and 4-hydroxyproline (Hyp), respectively (2,3). Collagen-derived Hyp-containing peptides show a variety of physiological activities (4-9): Pro-Hyp and alanine (Ala)-Hyp-Gly promote cell proliferation in dermal fibroblasts, while Pro-Hyp, Ala-Hyp-Gly, and leucine (Leu)-Hyp-Gly enhance collagen secretion in pre-osteoblast cells (7,10). Hyp-Gly promotes myogenic differentiation and myotube hypertrophy (11). Leu-Hyp-Gly shows strong angiotensin-converting enzyme inhibitory activity (12). Pro-Hyp is shown to be generated by the degradation of endogenous collagen in granulation tissue to activate cells involved in tissue reconstruction/remodeling (13). The administration of gelatin hydrolysate produces a significant increase in the mean diameter of collagen fibrils in Achilles tendon (14). However, to date, no detailed study has explored the functional role of Hyp-containing peptides in tendon cell behavior. It also remains unknown whether the cellular uptake of collagen-derived peptides in tendon cells is a carrier-mediated process.

Tendon is a dense connective tissue composed of highly organized parallel and longitudinal collagen fiber bundles (15-17). Resident tendon cells (“tenocytes”) originate from multipotent mesenchymal cells and actively produce unique and tendon-specific ECM (18). Tendon stem/progenitor cells exist in normal adult human and mouse tendons (19). We have recently demonstrated that tendon progenitor cells but not residential tenocytes play a central role in the repair following adult tendon injury (20). Scleraxis (SCX) is a basic helix-loop-helix transcription factor that has been identified as a highly specific marker for tendon and ligament cells (21). The transcription of *type I collagen* (*Col1a1* and *Col1a2)* genes is specifically and directly controlled by SCX in tenocytes and cardiac fibroblasts (22-24). The tenogenic marker Scx and the chondrogenic marker SRY-box 9 (SOX 9) are known to coordinately regulate the determination of cellular lineages during embryonic development (25). Adult tenocytes in tendon/ligaments with osteoarthritis acquire chondrogenic potential, showing down-regulation of SCX and upregulation of SOX 9 (20,26). Mohawk (MKX) and tenomodulin (TNMD) are also tenogenic markers during development. MKX is a transcription factor that regulates the expression of tendon-related genes such as *Scx* and *type I collagen* (27-29). TNMD is a type II transmembrane glycoprotein that is predominantly expressed in tendons and ligaments in the late stage of tendon development (30). Nevertheless, no studies to date have identified a requirement for Hyp-containing peptides in tenogenic differentiation and tenocyte maturation.

The major ECM component in tendon tissues is type I collagen (31). We have demonstrated that there are at least two independent mechanisms underlying type I collagen fibril re-organization following adult tissue injury, a fibronectin-dependent mechanism and a transforming growth factor-beta (TGF-β)/ type V collagen-dependent mechanism (32,33). Integrins are ECM receptors composed of transmembrane αβ heterodimeric subunits that mediate the organization of ECM, focal

contacts and actin-containing cytoskeleton (34,35). A knowledge of complex integrin-mediated “outside-in” and “inside-out” signal transduction is crucial to our understanding of how integrin is associated with extracellular ligands and/or intracellular effector molecules and consequently regulates cellular behavior (36-38).

Cell migration is a dynamic process which is important for a variety of biological processes, including embryonic development, tissue repair, immune response, and tumor invasion (39,40). Integrin engagement has a significant impact in migrating cells (41,42): it is associated with the extension of lamellipodial and filopodial protrusions at the leading edge, where newly polymerizing actin fibers and activated but unligated integrins are clustered (43). Growing evidence reveals that the persistence of lamellipodia is a critical factor in steering cell migration and regulating cell directionality (44). The directionality of cell migration is defined as the displacement divided by the total path length of the cell; thus, if the cell is migrating more randomly, the cell directionality decreases and *vice versa* (45).

It remains to be elucidated how Hyp-containing peptides alter tendon cell phenotypes *in vitro*, and the precise underlying molecular mechanisms are unknown. In the present study, we hypothesized that Hyp-containing peptides have functional roles in improving cellular homeostasis in tendon cells. We recently established adult tenocyte and tendon progenitor cell lines from mouse Achilles tendon tissues that express the *scx* promoter-driven green fluorescent protein (GFP) as a marker, in which the expression of SCXGFP is observed when the cells differentiate into mature tenocytes (20,46). Here, we explore the phenotypic changes in mouse tendon cells mediated by Hyp-containing peptides.

Results

Hyp-containing peptides enhance cell proliferation in adult tenocytes and tendon progenitor cells.

The phenotypic contribution of Hyp-containing peptides to tendon cells has not yet been studied. Micro- to millimolar concentrations of collagen-derived peptides induce chemotactic activity in a variety of cell types *in vitro* (47,48), and food-derived collagen peptides in human peripheral blood are present in micromolar concentrations (49,50). To study the cell response to Hyp-containing peptides, cells were initially cultured with four different Hyp-containing peptides at micromolar concentrations (Ala-Hyp-Gly, Leu-Hyp-Gly, Hyp-Gly, and Pro-Hyp; 80 μg/mL [289–462 μM]) in medium containing 5% dialyzed fetal bovine serum (FBS). Among the peptides examined, Pro-Hyp showed the greatest activity in adult tenocytes and tendon progenitor cells at day 3, which was accompanied by significant upregulation of *type I collagen* and *fibronectin* mRNA levels (Suppl. Fig. 1A, 1B). mRNA of the tendon-specific transcription factor *Scx* was also significantly upregulated at day 6 (Suppl. Fig. 1B). Next, to explore the cell response to Hyp-containing peptides, the dose-response to Pro-Hyp peptide was studied focusing on micromolar concentrations (0.1–500 μg/mL [0.5–2,200 μM]). We found that higher concentrations, 200 and 500 μg/mL, showed more effective cell proliferation activity in both tenocytes and tendon progenitor cells (Fig. 1A). More specifically, Pro-Hyp significantly upregulated cell proliferation activity in both cell types in a concentration-dependent manner (Fig. 1B). Treatment of cells with the same concentration of L-Pro or L-Hyp did not produce any changes (data not shown). These results indicate that Pro-Hyp is the most active peptide in tendon cells. Hereafter, we focused on cellular phenotypes induced by 200 and 500 μg/mL Pro-Hyp.

Uptake of Pro-Hyp into adult tenocytes

The important unsolved questions are whether Pro-Hyp is directly associated with specific receptors and activates subsequent intracellular signaling cascades, or carrier-mediated intracellular uptake of Pro-Hyp occurs, which results in the activation of inside-out signaling cascades. To study the potential for Pro-Hyp uptake into adult mouse tenocytes, a time-course assay was carried out using a stable isotopically labeled Pro-Hyp, $^{13}C_5{}^{15}N_1$-Pro-Hyp (SI-Pro-Hyp). SI-Pro-Hyp uptake into adult mouse tenocytes exhibited transporter-mediated uptake kinetics with a linear phase of uptake (about 30 min) (Fig. 2A). Importantly, this uptake was significantly decreased at 4°C (Fig. 2B). To further investigate this process, a kinetic analysis was performed at 37°C in the linear phase of uptake at a fixed 30-min time point with increasing Pro-Hyp concentrations ranging from 200−30,000 μg/mL. However, saturation was not observed up to 30,000 μg/mL Pro-Hyp, and Pro-Hyp uptake did not follow Michaelis−Menten kinetics (data not shown). Glycylsarcosine (Gly-Sar), a typical substrate for peptide transporter 1 (PEPT1) (51), did not inhibit Pro-Hyp uptake in adult tenocytes (data not shown), indicating that the uptake of Pro-Hyp is not mediated by PEPT1.

Recently, a series of studies on cell-penetrating peptides have revealed that these peptides are incorporated into cells via various non-selective pathways such as endocytosis and direct translocation pathways (52-54). To study further the localization of internalized Pro-Hyp in adult tenocytes, subcellular localization analysis was carried out using SI-Pro-Hyp immediately after uptake. Interestingly, 75.5% of total SI-Pro-Hyp incorporated into cells was localized in the cytosolic fraction, 16.4% in the membranes, 5.8% in the cytoskeleton, and 2.3% in the nucleus (Fig. 2C) at 60 min after Pro-Hyp treatment, suggesting that tenocytes internalize Pro-Hyp through multiple pathways, including transporters and non-selective pathways.

Pro-Hyp promotes tenogenic differentiation and maturation

We next explored the extent of the contribution of Pro-Hyp to differentiation and maturation in adult tenocytes and tendon progenitor cells. At day 6, mRNA of the tenogenic marker *Scx* was significantly upregulated (up to ~4.0-fold increase compared to untreated control), whereas mRNA of the chondrogenic marker *Sox 9* was significantly downregulated (~0.3-fold compared to untreated control) in both tenocytes and tendon progenitor cells. Thereafter, *Scx* mRNA levels were markedly downregulated by day 11 (Fig. 3A). The mRNA levels of another tenogenic marker, *mohawk*, and of the tendon maturation marker *tenomodulin* (55) were upregulated (up to ~40-fold increase compared to untreated control) at a later stage (day 11) in both tenocytes and tendon progenitor cells (Fig. 3A). The expression levels of *type II collagen* and *aggrecan* mRNA in both cell types were undetectable even after treatment with Pro-Hyp (data not shown).

The protein expression of *Scx* promoter-driven GFP (SCXGFP) (20,46) was further analyzed under the fluorescence microscope during the time course. From day 4 after treatment of adult tenocytes with Pro-Hyp, SCXGFP became visible, suggesting promotion to more mature tenocytes (Fig. 3B). Although there was only weak induction, SCXGFP had also become visible in tendon progenitor cells by day 10, confirming promotion to tendon-lineage differentiation by Pro-Hyp (Fig. 3B). SCXGFP was not induced in untreated cells used as negative controls (Fig. 3B).

Pro-Hyp upregulates ECM production and type I collagen assembly *in vitro*

SCX is known to directly regulate the *Col1a1* and *Col1a2* genes in tendon cells (24). Since *Scx* is upregulated in response to Pro-Hyp dipeptide, the functional link between Pro-Hyp and ECM production was addressed. Adult tenocytes and tendon progenitor cells treated with Pro-Hyp for 3 days showed significantly higher mRNA expression of *type I collagen* and the type I collagen-nucleation factor *fibronectin*, whereas another nucleation factor, *type V collagen* (33,56), was unchanged (Fig. 4A). The protein production of type I collagen and fibronectin was also significantly increased in cellular lysates in response to Pro-Hyp in both cell types (Fig. 4B), whereas type V collagen production did not show marked changes (data not shown). Pro-Hyp also affected (up to ~1.5-fold increase) the amounts of type I collagen secreted into the culture medium (data not shown). Collagen network organization is a critical process that occurs upon tissue damage and/or remodeling (57,58). We further explored the functional role of Pro-Hyp in the structural integrity of

collagen *in vitro*. Phase-contrast image analysis showed that cells formed similar dense sheet-like structures with or without peptide treatment. Immunofluorescence analysis revealed that treatment of adult tenocytes with 500 μg/mL Pro-Hyp resulted in a significantly denser and thicker type I collagen fibril network organization compared to untreated controls (Fig. 4C). We have recently demonstrated that there are at least two independent mechanisms of type I collagen assembly, fibronectin-mediated and type V collagen-mediated (33). Thus, ~50% increase of fibronectin production in response to 500 μg/mL Pro-Hyp shown above may reflect the significant increase of type I collagen organization in adult tenocytes.

Proteomics analysis and activation of extracellular signal-regulated kinase (ERK) in response to Pro-Hyp

It is not yet known what the functional links are between Pro-Hyp and cell cycle progression or between cell proliferation and other signaling pathways. We next sought to understand how Pro-Hyp dipeptide modulates adult tenocyte behavior at an early time point using proteomics as a global screening tool. Liquid chromatography–mass spectrometry (LC-MS)/MS identified 3006 proteins across all samples (the mass spectrometry proteomics data have been deposited to the ProteomeXchange Consortium via the PRIDE (59) partner repository with the dataset identifier PXD023176). After exposure to Pro-Hyp for 6 hrs, 26 proteins were significantly increased and 290 significantly decreased compared to the time-matched control sample, as revealed by ANOVA. Since the number and significance of the changes were small, the data were evaluated by functional annotation and Ingenuity pathway analysis (IPA). IPA identified molecular transport, cellular assembly and organization, and cellular movement as predicted linked-network pathways at this early time point in adult tenocytes (Suppl. Table 2 and Suppl. Fig. 2). Therefore, these events and related signaling molecules were investigated further.

The classical ERK family (p42/44 mitogen-activated protein kinase [MAPK]; shown in Suppl. Fig. 2B) is known to be an intracellular checkpoint for cellular mitogenesis. In cultured cells, mitogenic stimulation by growth factors correlates with stimulation of p42/44 MAPK, indicating that the ERK cascade plays a pivotal role in the control of cell cycle progression (60). Therefore, the phosphorylation level of ERK was investigated during the time course. Treatment of tendon cells with 200 μg/mL Pro-Hyp resulted in the significant upregulation of phospho-ERK: the maximum upregulation of phospho-ERK (~6.0-fold increase) was found at 24 hrs after treatment in adult tenocytes and at 12 hrs after treatment in tendon progenitor cells, compared to untreated time 0 (Fig. 5A). These findings indicate the involvement of ERK signaling pathways in tendon cells treated with Pro-Hyp.

Pro-Hyp-driven cell motility

Accumulating evidence has revealed that ERK signaling is one of the critical regulators of cell motility, although it is classically known as an important regulator of cell proliferation, differentiation and survival through the regulation of gene expression (61). Since IPA identified cellular movement

as one of the predicted linked-network pathways in response to Pro-Hyp (Suppl. Fig. 2B) and Hyp-containing peptides show chemotactic activity in a variety of cell types (4,47,48,62), a transwell migration assay was next performed using Boyden chambers. Adult tenocytes and tendon progenitor cells exhibited significantly enhanced chemotactic activity (up to ~3.3-fold increase) in response to Pro-Hyp (Fig. 5B).

During directional migration, cells move in response to an extracellular chemotactic signal or intrinsic cues provided by the basic motility machinery (63). In order to visualize the detailed morphological changes that cells undergo during Pro-Hyp-induced migration, time-lapse image analysis of adult tenocytes was carried out. Elongated lamellipodia-like protrusions, which are broad, flat protrusions at the leading edge of cells moving on a flat substratum (44), were observed at 11 hrs after treatment with Pro-Hyp (Fig. 6A, Suppl. Fig. 3). The numbers of cells with lamellipodia-like protrusions increased significantly (~1.78-fold compared to untreated cells; Fig. 6A). In trajectory plots analyzing migrating tracks, cells treated with Pro-Hyp clearly demonstrated increased directional persistence compared to untreated controls (Fig. 6B): this resulted in a significantly increased (~2.0-fold) number of cells with directional cell movement (cells that migrate with a directionality ratio of more than 0.8; see details in Materials and methods) (Fig. 6C). Furthermore, the numbers of cells i) migrating more than 10 μm and ii) migrating more than 5 μm/hr in response to Pro-Hyp were also significantly increased (Fig. 6C).

Since the engagement of active integrin is known to be important for protrusion formation with reorganization of the actin cytoskeleton (41,42), the functional link between Pro-Hyp dipeptide and integrin/actin cytoskeletal organization was addressed. Integrin expression profiles in primary tenocytes from adult mouse Achilles tendon as assessed by fluorescence-activated cell sorting (FACS) analysis revealed that adult tenocytes were positive for β1, α1, α5, α11, and αv integrins, and very weak or negative for α6, α2, and β3 integrins (Suppl. Fig. 4). There is experimental evidence that cell-matrix adhesions containing α5β1 integrin are highly dynamic, whereas adhesions containing αvβ3 are more static (64). We therefore explored the cellular distribution of the most ubiquitously expressed integrin subunit, β1, which was positive in tenocytes (using antibody 9EG7, which recognizes an extracellular epitope of ligand-inducible active β1 (65)). Immunofluorescence analysis demonstrated that treatment of adult tenocytes with 500 μg/mL Pro-Hyp resulted in a significantly increased number (~2.2-fold) of active β1-integrin-containing focal contacts and a significantly increased thickness (~2.8-fold) of peripheral F-actin fibrils compared to untreated controls (Fig. 7A).

Finally, the functional links between Pro-Hyp induced cellular phenotypes and ERK- and β1-integrin-mediated signaling were addressed. Pretreatment of adult tenocytes with mitogen-activated protein kinase kinase (MEK)1/2 inhibitor PD98059 completely abrogated Pro-Hyp-mediated increased migratory activity ($P < 0.001$), and the magnitude of migration was decreased to a level slightly less than that of controls not treated with Pro-Hyp (Fig. 7B). In addition, although to a lesser degree, pretreatment of adult tenocytes with the α5β1-integrin antagonist ATN-161 (66) resulted in a reduction (~64.2%; $P < 0.001$) in Pro-Hyp-mediated cell migration. Furthermore, ATN-161

significantly inhibited (~76.8% inhibition) uptake of Pro-Hyp into adult tenocytes (Fig. 7C), suggesting Pro-Hyp as α5β1-integrin ligand and mediation of outside-in signaling. Thus, taken together, these findings indicate the involvement of ERK-mediated and β1-integrin-mediated signaling in Pro-Hyp-induced cellular phenotypes such as cell migration activity in adult tendon cells.

Discussion

Although a previous observation suggests a functional role of specific collagen-derived peptides in the biosynthesis of matrix molecules of tendon and ligament cells (67), as of today, no molecular framework exists for understanding the mechanisms that regulate adult tendon cell phenotypes in response to those peptides. Our current study on tendon cells provides compelling evidence for the following propositions: 1) Among the peptides examined, Pro-Hyp is the most effective one to induce cellular phenotypes, and the cellular uptake of Pro-Hyp is suggested to occur by multiple pathways; 2) Pro-Hyp promotes differentiation/maturation of tendon cells, enhances cell proliferation with significantly upregulated ERK-phosphorylation, and promotes type I collagen assembly *in vitro*; 3) Cells treated with Pro-Hyp demonstrate significantly increased cell motility and migration velocity, which are accompanied by elongated lamellipodial protrusions with increased active β1-integrin-containing focal contacts and thicker peripheral F-actin fibrils; and 4) Pro-Hyp-mediated chemotactic activity shows significant reduction on treatment of cells with the MEK1/2 inhibitor PD98059 or the α5β1-integrin antagonist ATN-161. Furthermore, ATN-161 significantly inhibits uptake of Pro-Hyp into adult tenocytes.

Possible mechanisms of the cellular uptake of Pro-Hyp in tendon cells

A growing body of evidence indicates novel and unique roles of transporters in regulating metabolites and signaling molecules, and in communication between organs and organisms (68). Little insight into mechanisms of the cellular uptake of Hyp-containing peptides has emerged from pharmacokinetic studies in tendon cells. In the present study, the intracellular uptake of Pro-Hyp in tendon cells is suggested to be a carrier-mediated process. Pro-Hyp-specific transporters have not yet been identified, but several candidate molecules have been suggested. One example is the peptide transporter PEPT1, which can transport di- and tri-peptides (51). However, we found that glycylsarcosine (Gly-Sar), a typical substrate for PEPT1, did not inhibit Pro-Hyp uptake in adult tenocytes. Another example, the peptide/histidine transporter PHT-1, mediates di- and tri-peptide uptake, and co-administration of histidine partially inhibits Hyp-Gly-induced cellular differentiation (11). Our subcellular localization analysis showed that Pro-Hyp peptide was incorporated into not only the cytosol but also the membranes/organelles, the cytoskeleton, and the nucleus, and α5β1-integrin antagonist ATN-161 significantly inhibited uptake of Pro-Hyp. These findings strongly suggest the existence of more than one mechanism for the intracellular incorporation of Pro-Hyp, i.e., not only selective uptake mediated by transporters but also non-selective uptake mediated by endocytosis (52-54). The detailed mechanisms underlying the uptake of Hyp-containing peptides remain to be elucidated in tendon cells.

Pro-Hyp/phospho-ERK/Scx and Pro-Hyp/phospho-ERK/integrin axes in tendon cells

Collagen-derived Hyp-containing peptides can promote osteogenesis and chondrogenesis *in vitro* (8,9,69). Recent observations show that both fibroblast growth factor (FGF)/mitogen-activated

protein kinase (MAPK)-ERK and TGFβ/Smad2/3 signaling pathways are necessary and sufficient for *Scx* expression in chick undifferentiated limb cells, whereas inhibition of the MAPK-ERK signaling pathway is sufficient to activate *scx* in developing mouse limb progenitors (70,71). SCX directly regulates the transcription of *type I collagen* (*Col1a1* and *Col1a2)* genes in tendon cells (24) and has been shown to be necessary and sufficient for *Tnmd* expression (21,30,72). This experimental evidence supports our current findings demonstrating that Pro-Hyp significantly upregulates *Scx*, *Mkx*, and *Tnmd* expression and promotes tenogenic differentiation/maturation, which results in a significant increase in type I collagen production and network organizations brought about by tendon cells. In contrast, *Scx*-null progenitors display higher chondrogenic potential with upregulation of *Sox 9* (20). These findings document the counteracting effects of lineage-specific transcription factors on cellular differentiation/maturation by Pro-Hyp.

There is evidence that, when integrins are activated by ligands, endocytosis pathways through the recycling endosome are activated (73,74). Our present findings have demonstrated ~64.2% reduction in Pro-Hyp-mediated tenocyte migration by ATN-161. Furthermore, ATN-161 has significantly inhibited uptake of Pro-Hyp into adult tenocytes, although not complete inhibition (~76.8%). These findings support a scenario that Pro-Hyp could mainly function as a ligand for α5β1-integrin and activate downstream ERK cascades by outside-in signaling.

Although an earlier study indicates that Pro-Hyp can abolish the suppression of the growth of skin fibroblasts on collagen gel rather than acting as a growth factor (4), the underlying molecular mechanisms have not been addressed. We have shown here the links between cell proliferation and phospho-ERK upregulation in tendon cells treated with Pro-Hyp. Recent lines of evidence have revealed the engagement of integrin-mediated inside-out signaling axes in cellular behaviors, including mediation by the MEK/ERK signaling pathway (75-77). The signaling axis by which intracellularly transported Pro-Hyp mediates enhanced cell proliferation through upregulated phospho-ERK remains to be elucidated.

Upregulation of Pro-Hyp-driven cell migration activity in tendon cells

Although the recent observation of treating cells with mitomycin C suggests that Pro-Hyp enhances the growth of skin fibroblasts but does not enhance their motility (4), it is not clear whether Pro-Hyp can alter cell motility with the engagement of active integrins and actin re-organization in tendon cells. Integrins affect a multitude of signal transduction cascades in the control of cell proliferation and differentiation, migration, and the production of ECM (34,36). Cell migration requires membrane protrusion at the cell front, and integrins mediate actin polymerization and organization at the leading edge of migrating cells (78). Our finding that the numbers of cells with lamellipodial protrusions were significantly increased in the presence of Pro-Hyp is consistent with the fact that lamellipodial protrusion is powered by actin polymerization, which in turn is mediated by the nucleation of branched actin networks induced by actin-related protein 2/3 (Arp2/3) (44) and by the small GTPases Cdc42 and Rac (79). The next question will be which cascades are triggered as the driving machinery to promote cell migration and actin reorganization in response to Pro-Hyp (80).

Hyp-containing peptides for translational medicine

Adult tendon injury is a difficult clinical problem. It occurs frequently, and injured tendon heals very slowly and is rarely restored to its normal undamaged state (81-83). Tendon disorders are thus highly debilitating and painful (81). Growing evidence demonstrates that, in response to injury, Pro-Hyp is locally generated by the degradation of endogenous collagen at the wound site to activate cells involved in tissue reconstruction/remodeling ((84,85), reviewed in (13)). Collagen-derived hydrolysates can promote the production of type III and type I collagen and proteoglycan in tendon/ligament cells *in vitro* and increase the average collagen fibril diameter in both normal and injured tendons *in vivo* (14,67,86). Pro-Hyp is identified as a major constituent of food-derived collagen in human blood after oral ingestion of gelatin hydrolysate (49,50). Clinically, oral supplementation of specific collagen peptides combined with calf-strengthening exercises enhances function and reduces pain in Achilles tendinopathy patients (87). Our current findings demonstrate several functional benefits of Pro-Hyp dipeptide at rather high concentrations (200–500 μg/mL [880–2,200 μM]) in tendon cell behavior without any cytotoxic effects. These findings, taken together, make it tempting to speculate that local injections of Hyp-containing peptides could be suitable therapeutic candidates for improving the slow-healing response to adult tendon injury by promoting tendon cell differentiation/maturation and/or enhancing collagen fibrillogenesis following injury. Detailed analysis of the dynamic properties of collagen-derived peptides could shed the light on their potential application to translational medicine.

Materials and Methods

Cell culture

Adult mouse tendon progenitor cells and adult mouse tenocyte lines were established from primary cell cultures of Achilles tendons from 10-to-12-wk-old *Scx(flox/flox)/ScxGFP/p53(-/-)* and *Scx(flox/flox)/ScxGFP/p21(-/-)* mice, as described previously (20,46). Tendon progenitors and tenocytes were maintained in Minimum Essential Medium Eagle Alpha Modification medium (MEM-α) and Dulbecco's modified Eagle's medium (DMEM), respectively, supplemented with 10% FBS and 1% non-essential amino acids. All Hyp-containing peptide experiments were performed using culture medium containing 5% dialyzed FBS. In studies performed over 3 or more days, cultures were re-dosed with peptides daily. Primary tenocyte cultures from adult mouse Achilles tendons were performed as described elsewhere (46).

Reagents and antibodies

Pro-Hyp and Hyp-Gly peptides were purchased from Bachem (Switzerland), and other peptides were custom synthesized by AnyGen (Korea). The following antibodies were used: rabbit polyclonal antibody (pAb) against mouse type I collagen (Chemicon: this antibody shows less than 0.1% reactivity with mouse collagen types II and IV in addition to 1.0% reactivity with mouse collagen type III); rabbit pAb against mouse fibronectin (Chemicon: this antibody has cross-reactivity to bovine fibronectin, and shows less than 0.1% reactivity with mouse laminin and collagen types I, III, and IV by radioimmunoassay); rabbit pAb against the C-telopeptide of the α1 chain of type I collagen (LF68; provided by Dr. Larry Fisher, NIH, USA); rabbit pAb (Abcam) and goat pAb (Thermo Fisher) against human type V collagen; mouse monoclonal antibody (mAb) against phospho-ERK1/2 (pT202/pY204) and rabbit pAb against total Erk (Cell Signaling); rat mAb against mouse integrin β1 (clone 9EG7) (65), hamster mAbs against mouse integrin β1 (clone Ha2/5), mouse integrin α1 (clone Ha31/8), and mouse integrin α2 (clone Ha1/29); rat mAbs against mouse integrin α5 (clone 5H10-27), mouse integrin α6 (clone GoH3), and mouse integrin αv (clone RMV-7) and hamster mAb against mouse integrin β3 (clone 2C9.G2) (all from Pharmingen); α11 (rabbit pAb; provided by Dr Donald Gullberg, Univ. Bergen, Norway); rabbit pAb against human calnexin (sc-11397; Santa Cruz); rabbit pAb against human Histone H1.0 (GeneTex); mouse mAb against human vimentin (clone VIM-13.2; Sigma); mouse mAb against α-tubulin (clone B-5-1-2; Sigma); and mouse mAb against rabbit glyceraldehyde-3-phosphate dehydrogenase (GAPDH; clone 3H12; MBL). Peroxidase-conjugated donkey anti-mouse and anti-rabbit IgG were from Jackson ImmunoRes Laboratories Inc. Alexa Fluor 488 goat anti-rat IgG, Alexa Fluor 568 goat anti-rabbit IgG and Alexa Fluor 568 Phalloidin were from Invitrogen. Platelet-derived growth factor (PDGF) from porcine platelets and human recombinant transforming growth factor-beta1 (TGF-β1) were from R&D Systems. MEK1/2 inhibitor PD98059 (IC_{50} = 2 μM) was from Calbiochem, and α5β1 integrin antagonist ATN-161 was from Tocris.

Uptake and subcellular localization analysis of Pro-Hyp in adult mouse tendon cells

Adult tenocytes were seeded at 3 × 10^5 cells/well in 6-well plates and cultured for 12 hrs in growth medium. The growth medium was then replaced with transport buffer consisting of Hanks balanced salt solution (HBSS), 25 mM HEPES, and 0.1% (w/v) bovine serum albumin (BSA) at pH 7.4 with $^{13}C_5{}^{15}N_1$-Pro-Hyp (SI-Pro-Hyp; 200 µg/mL) or Pro-Hyp (200−30,000 µg/mL). After incubation at 37°C for various time periods, cells were washed three times with ice-cold phosphate-buffered saline (PBS), and cell lysates were harvested in 0.1% Triton X-100 containing protease inhibitor cocktail. After one freeze-thaw cycle and freeze-drying of the solution, the sample was reconstituted with 0.1% formic acid, and a previously developed internal standard mixture containing $^{13}C_5{}^{15}N_1$-Pro-$^{13}C_5{}^{15}N_1$-Hyp (2SI-Pro-Hyp) was added as an internal standard (88). Then the sample was subjected to LC–MS analysis in multipole reaction monitoring mode for quantification of SI-Pro-Hyp (*m/z* 235.2→75.1) and Pro-Hyp (*m/z* 229.2→70.1), whose concentrations were determined by the peak area ratio relative to 2SI-Pro-Hyp (*m/z* 241.2→75.1) as described previously (88).

To study the effect of the α 5β1-integrin antagonist ATN-161 on uptake of SI-Pro-Hyp in adult tenocytes, cells were preincubated with ATN-161 (100 µM; (89)) for 60 min. Then the uptake assay was performed using 200 µg/mL SI-Pro-Hyp at 37°C for 60 min as described above. We confirmed that the concentration of ATN-161 used did not affect adult tenocyte proliferation (data not shown).

In subcellular localization analysis, adult tenocytes were seeded at 3 × 10^5 cells/well in 6-well plates and cultured for 12 hrs in growth medium. The growth medium was then replaced with transport buffer containing 200 µg/mL of SI-Pro-Hyp. After incubation at 37°C for 60 min, cells were washed three times with ice-cold PBS. Cells were sequentially extracted by the Calbiochem® ProteoExtract® Subcellular Proteome Extraction Kit (Millipore) according to the manufacturer's instructions. The accuracy of fractionation was confirmed by Western blot analysis using antibodies against GAPDH (MBL; cytosolic), Calnexin (Santa Cruz; membrane/organelle), Histone-1 (Genetex; nulcear), and Vimentin (Sigma; cytoskeletal) (Suppl. Fig. 5). After addition of the internal standard mixture containing 2SI-Pro-Hyp, the extracted samples were diluted with 0.1% formic acid and subjected to LC-MS analysis.

Immunofluorescence

Immunofluorescence studies were performed as described previously (90). In type I collagen network and active β1-integrin and F-actin staining, images were captured with the same gain, offset, magnitude, and exposure time. For quantification of type I collagen network-positive areas, a minimum of four different cell images werre randomly selected and their intensities quantified using ImageJ software (version 1.48; National Institutes of Health) (56).

Real-time PCR

Real-time PCR was performed as described elsewhere (46,91). The following primers were used: *Scx* forward, 5'-GAGACGGCGGCGAGAAC-3'; *Scx* reverse, 5'-TTGCTCAACTTTCTCTGGTTGCT-3'; *Sox9* forward, 5'-CGGCTCCAGCAAGAACAAG-3'; *Sox9* reverse, 5'-TGCGCCCACACCATGA-3';

Mkx forward, 5'-GCAGAATGGAGGGAAGGTAAG-3'; Mkx reverse, 5'-GGTTGTCACGGTGCTTGTA-3'; *Tnmd* forward, 5'-GAAACCATGGCAAAGAATCCTCCAGAG-3'; *Tnmd* reverse, 5'-TTAGACTCTCCCAAGCATGCGGGC-3'; *collagen type I* (*Col1a1)* forward, 5'-TTTGTGGACCTCCGGCTC-3'; *collagen type I* (*Col1a1)* reverse, 5'-AAGCAGAGCACTCGCCCT-3'; *collagen type V* (*Col5a1)* forward, 5'-AGGACCACACAGGGAAGC-3'; *collagen type V* (*Col5a1)* reverse, 5'-CTTGTAGACACTGAGAGCAATTCG-3'; *fibronectin* forward, 5'-GGCTCCAGATCCATCCAACAC-3'; *fibronectin* reverse, 5'-GACAGCCACTTTCACAGACAG-3'; *collagen type II (Col2a1)* forward, 5'-AGAACAGCATCGCCTACCTG-3'; *collagen type II (Col2a1)* reverse, 5'-CTTGCCCCACTTACCAGTGT-3'; *aggrecan* forward, 5'-GAGGAGAGAACTGGAGAAG-3'; *aggrecan* reverse, 5'-GGCGATAGTGGAATACAA-3'; 18S rRNA forward, 5'-GGCGACGACCCATTCG-3'; and 18S rRNA reverse, 5'-ACCCGTGGTCACCATGGTA-3'. All samples were analyzed at least in triplicate. After the reactions, the specificity of amplification in each sample was confirmed by dissociation analysis, showing that each sample gave a single melting peak. mRNA levels were normalized to the level of 18S rRNA.

Western blot analysis

Western blot analyses were performed as described elsewhere (33). In some immunoblot analyses, samples were transferred onto an Immobilon-FL polyvinylidene fluoride (PVDF) membrane (Millipore Corp.) and probed with primary and IRDye 800CW- or IRDye 680-conjugated secondary antibodies (LI-COR Biosciences). Immunoreactive bands were detected using the Odyssey IR Imaging System (LI-COR Biosciences).

Proteomics analysis

Adult tenocytes were treated with or without 500 µg/mL of Pro-Hyp for certain time periods, then washed, scraped and pelleted in phosphate buffer (pH 7.4). Subsequently, cells were resuspended in a volume of 0.5 M tetraethylammonium bromide (TEAB)/0.1% SDS equivalent to the volume of the cell pellet, subjected to one freeze-thaw cycle, sonicated and centrifuged. Samples were prepared in duplicate and randomized across 3 iTRAQ experiments, with a pool of all the samples acting as a common denominator in each of the iTRAQ runs. Samples containing 100 µg protein were denatured, reduced and treated with methyl methanethiosulfonate according to the manufacturer's protocol (Sciex), before being labelled with 8-plex isobaric tags for absolute and relative quantification (iTRAQ), pre-fractionated by cation exchange chromatography and analyzed on a Triple TOF 6600 mass spectrometer (Sciex) as previously described (92). Briefly, 40 desalted fractions were reconstituted in 0.1% formic acid and 5 µl of each was loaded onto the column. Peptides were separated by in-line reversed phase chromatography on an Eksigent nanoLC 415 (nanoACQUITY UPLC Symmetry C18 Trap Column and an ACQUITY UPLC Peptide BEH C18 nanoACQUITY Column; Waters, UK). A gradient from 2−50% ACN/0.1% formic acid (v/v) over 90 min at a flow rate of 300 nL/min was applied. Spectra were acquired automatically in positive ion mode using information-dependent acquisition (Analyst TF 1.7.1. software; Sciex). Up to 25 MS/MS

spectra were acquired per cycle (approximately 10 Hz) using a threshold of 500 counts per sec and with dynamic exclusion for 20 sec. The rolling collision energy was increased automatically by selecting the iTRAQ check box in Analyst, and manually by increasing the collision energy intercepts by 5. Data were searched using ProteinPilot 5.0 (Sciex) and the Paragon algorithm (Sciex) against the SwissProt database (May 2019; 17,013 mouse entries) with methylthio as a fixed modification of cysteine residues and biological modifications allowed. The mass tolerance for precursor and fragment ions was 10 ppm. The data were also searched against a reversed decoy database and proteins lying within a 1% global false discovery rate were included in further analyses. Data from the 3 iTRAQ experiments were merged using RStudio V.1.0.143 and only proteins for which there were values in all samples were taken forward. ANOVA was performed on the natural log transformed data using Partek Genomics Suite 7.18, with iTRAQ experiment and treatment as variables. Functional annotation cluster analysis was performed on altered proteins using the Database for Annotation, Visualization and Integrated Discovery (DAVID), with the full list of proteins identified in the combined iTRAQ data as the background list (93,94). In addition, functional pathway prediction activity, upstream regulator analysis and network analysis was performed on the same list of genes using the Ingenuity Pathway Analysis (IPA) software. Functional pathway prediction activity is designed to infer which functions may be activated or repressed. IPA is able to infer a functional response by comparing the observed change in protein expression with prior knowledge of expected effects between regulatory and effector genes stored in the Ingenuity Knowledge database. We applied this approach to identify which biological functions were likely to be activated or repressed as well as to infer which proteins that may not have been detected by the proteomics analysis may be responsible for driving the observed differences in the proteomic profile (upstream regulator analysis). Network Analysis instead identified protein interactions that link the list of input proteins.

Cell migration

Cell migration assays were performed in modified Boyden chambers containing Nucleopore polycarbonate membranes (5-µm pore size; Costar Corp., Cambridge, MA) as described previously (65,95). Briefly, the filters were soaked overnight in a 100 µg/mL solution of gelatin. Chemoattractants in culture medium were added to the lower compartment of the chambers. Cells suspended in culture media were introduced into the upper compartment of the chamber. The chambers were then incubated for 6 hrs at 37°C. The filters were fixed and stained, and the cells that had migrated to the lower surface were counted.

To study the effect of the MEK1/2 inhibitor PD98059 (IC_{50} = 2 µM) and the α5β1-integrin antagonist ATN-161 on Pro-Hyp-mediated cell migration in adult tenocytes, cells were preincubated for 1 h and treated with PD98059 (20 µM) or ATN-161 (100 µM; (89)). Then migration assays were performed as described above. We confirmed that the concentration of the inhibitors used did not affect adult tenocyte proliferation (data not shown).

Time-lapse microscopic analysis

Adult tenocytes (20,000 cells) were plated on one compartment of 3.5-cm four-compartment dishes. Cells were initially cultured for the first 4 hrs without peptides, then treated with 200 or 500 µg/mL of Pro-Hyp and cultured for a further 11 hrs. During time-lapse assays, cells were imaged every 10 min for 15 hrs on a Zeiss LSM 710 confocal microscope with incubation conditions set to 37 °C and 5 % CO_2. The time-lapse settings were under transmitted light, with a 10× NA 0.45 objective, 1% laser intensity (488-nm line), 251 Master Gain, 512 × 512-pixel size. Six non-overlapping regions of interest were randomly selected for analysis (at least 36 cells under each set of condition). We defined directional-movement-positive cells as cells that migrated with a directionality ratio of more 0.8 (displacement divided by total cell movement) (96).

Data presentation and statistical analysis

All experiments were performed at least in triplicate on separate occasions, and the data shown were chosen as representative of results consistently observed. Results are presented as means ± standard deviation (S.D.). Differences between groups were analyzed using the two-sided Student's *t*-test on raw data. In cases where more than two groups were compared, one-way ANOVA and Dunnett's post-hoc test, or two-way ANOVA and Tukey's post-hoc test were used. A p value of < 0.05 was considered significant. All ANOVA data are shown in Suppl. Table 1.

Data Availability

All protein identifications are shown in Suppl. Table 3. All remaining data are contained within the article. The mass spectrometry proteomics data have been deposited to the ProteomeXchange Consortium via the PRIDE (https://www.ebi.ac.uk/pride/archive/) (59) partner repository with the dataset identifier PXD023176.

References

1. Ricard-Blum, S. (2011) The collagen family. *Cold Spring Harbor perspectives in biology* **3**, a004978
2. Brodsky, B., and Persikov, A. V. (2005) Molecular structure of the collagen triple helix. *Advances in protein chemistry* **70**, 301-339
3. Bächinger, H. P., Mizuno, K., Vranka, J. A., and Boudko, S. P. (2010) Collagen formation and structure. in *Comprehensive Natural Products II: Chemistry and Biology*, Elsevier Ltd. pp 469-530
4. Shigemura, Y., Iwai, K., Morimatsu, F., Iwamoto, T., Mori, T., Oda, C., Taira, T., Park, E. Y., Nakamura, Y., and Sato, K. (2009) Effect of Prolyl-hydroxyproline (Pro-Hyp), a food-derived collagen peptide in human blood, on growth of fibroblasts from mouse skin. *Journal of agricultural and food chemistry* **57**, 444-449
5. Wu, J., Fujioka, M., Sugimoto, K., Mu, G., and Ishimi, Y. (2004) Assessment of effectiveness of oral administration of collagen peptide on bone metabolism in growing and mature rats. *J Bone Miner Metab* **22**, 547-553
6. Tsuruoka, N., Yamato, R., Sakai, Y., Yoshitake, Y., and Yonekura, H. (2007) Promotion by collagen tripeptide of type I collagen gene expression in human osteoblastic cells and fracture healing of rat femur. *Biosci Biotechnol Biochem* **71**, 2680-2687
7. Ohara, H., Ichikawa, S., Matsumoto, H., Akiyama, M., Fujimoto, N., Kobayashi, T., and Tajima, S. (2010) Collagen-derived dipeptide, proline-hydroxyproline, stimulates cell proliferation and hyaluronic acid synthesis in cultured human dermal fibroblasts. *J Dermatol* **37**, 330-338
8. Kimira, Y., Ogura, K., Taniuchi, Y., Kataoka, A., Inoue, N., Sugihara, F., Nakatani, S., Shimizu, J., Wada, M., and Mano, H. (2014) Collagen-derived dipeptide prolyl-hydroxyproline promotes differentiation of MC3T3-E1 osteoblastic cells. *Biochemical and biophysical research communications* **453**, 498-501
9. Kimira, Y., Odaira, H., Nomura, K., Taniuchi, Y., Inoue, N., Nakatani, S., Shimizu, J., Wada, M., and Mano, H. (2017) Collagen-derived dipeptide prolyl-hydroxyproline promotes osteogenic differentiation through Foxg1. *Cellular & molecular biology letters* **22**, 27
10. Taga, Y., Kusubata, M., Ogawa-Goto, K., Hattori, S., and Funato, N. (2018) Collagen-derived X-Hyp-Gly-type tripeptides promote differentiation of MC3T3-E1 pre-osteoblasts. *Journal of Functional Foods* **46**, 456-462
11. Kitakaze, T., Sakamoto, T., Kitano, T., Inoue, N., Sugihara, F., Harada, N., and Yamaji, R. (2016) The collagen derived dipeptide hydroxyprolyl-glycine promotes C2C12 myoblast differentiation and myotube hypertrophy. *Biochemical and biophysical research communications* **478**, 1292-1297
12. Taga, Y., Hayashida, O., Ashour, A., Amen, Y., Kusubata, M., Ogawa-Goto, K., Shimizu, K., and Hattori, S. (2018) Characterization of Angiotensin-Converting Enzyme Inhibitory Activity of X-Hyp-Gly-Type Tripeptides: Importance of Collagen-Specific Prolyl Hydroxylation. *J Agric Food Chem* **66**, 8737-8743
13. Sato, K., Jimi, S., and Kusubata, M. (2019) Generation of bioactive prolyl-hydroxyproline (Pro-Hyp) by oral administration of collagen hydrolysate and degradation of endogenous collagen. *Int J Food Sci Technol* **54**, 1976-1980
14. Minaguchi, J., Koyama, Y., Meguri, N., Hosaka, Y., Ueda, H., Kusubata, M., Hirota, A., Irie, S., Mafune, N., and Takehana, K. (2005) Effects of ingestion of collagen peptide on collagen fibrils and glycosaminoglycans in Achilles tendon. *J Nutr Sci Vitaminol (Tokyo)* **51**, 169-174
15. Kjaer, M. (2004) Role of extracellular matrix in adaptation of tendon and skeletal muscle to mechanical loading. *Physiol Rev* **84**, 649-698
16. Benjamin, M., Kaiser, E., and Milz, S. (2008) Structure-function relationships in tendons: a review. *J Anat* **212**, 211-228
17. Zhang, G., Young, B. B., Ezura, Y., Favata, M., Soslowsky, L. J., Chakravarti, S., and Birk, D. E. (2005) Development of tendon structure and function: regulation of collagen fibrillogenesis. *J Musculoskelet Neuronal Interact* **5**, 5-21
18. Tozer, S., and Duprez, D. (2005) Tendon and ligament: development, repair and disease. *Birth Defects Res C Embryo Today* **75**, 226-236

19. Bi, Y., Ehirchiou, D., Kilts, T. M., Inkson, C. A., Embree, M. C., Sonoyama, W., Li, L., Leet, A. I., Seo, B. M., Zhang, L., Shi, S., and Young, M. F. (2007) Identification of tendon stem/progenitor cells and the role of the extracellular matrix in their niche. *Nat Med* **13**, 1219-1227
20. Sakabe, T., Sakai, K., Maeda, T., Sunaga, A., Furuta, N., Schweitzer, R., Sasaki, T., and Sakai, T. (2018) Transcription factor scleraxis vitally contributes to progenitor lineage direction in wound healing of adult tendon in mice. *J Biol Chem* **293**, 5766-5780
21. Murchison, N. D., Price, B. A., Conner, D. A., Keene, D. R., Olson, E. N., Tabin, C. J., and Schweitzer, R. (2007) Regulation of tendon differentiation by scleraxis distinguishes force-transmitting tendons from muscle-anchoring tendons. *Development* **134**, 2697-2708
22. Espira, L., Lamoureux, L., Jones, S. C., Gerard, R. D., Dixon, I. M., and Czubryt, M. P. (2009) The basic helix-loop-helix transcription factor scleraxis regulates fibroblast collagen synthesis. *Journal of molecular and cellular cardiology* **47**, 188-195
23. Bagchi, R. A., and Czubryt, M. P. (2012) Synergistic roles of scleraxis and Smads in the regulation of collagen 1alpha2 gene expression. *Biochimica et biophysica acta* **1823**, 1936-1944
24. Lejard, V., Brideau, G., Blais, F., Salingcarnboriboon, R., Wagner, G., Roehrl, M. H., Noda, M., Duprez, D., Houillier, P., and Rossert, J. (2007) Scleraxis and NFATc regulate the expression of the pro-alpha1(I) collagen gene in tendon fibroblasts. *J Biol Chem* **282**, 17665-17675
25. Asou, Y., Nifuji, A., Tsuji, K., Shinomiya, K., Olson, E. N., Koopman, P., and Noda, M. (2002) Coordinated expression of scleraxis and Sox9 genes during embryonic development of tendons and cartilage. *J Orthop Res* **20**, 827-833
26. Kumagai, K., Sakai, K., Kusayama, Y., Akamatsu, Y., Sakamaki, K., Morita, S., Sasaki, T., Saito, T., and Sakai, T. (2012) The extent of degeneration of cruciate ligament is associated with chondrogenic differentiation in patients with osteoarthritis of the knee. *Osteoarthritis Cartilage* **20**, 1258-1267
27. Anderson, D. M., Arredondo, J., Hahn, K., Valente, G., Martin, J. F., Wilson-Rawls, J., and Rawls, A. (2006) Mohawk is a novel homeobox gene expressed in the developing mouse embryo. *Dev Dyn* **235**, 792-801
28. Liu, H., Zhang, C., Zhu, S., Lu, P., Zhu, T., Gong, X., Zhang, Z., Hu, J., Yin, Z., Heng, B. C., Chen, X., and Ouyang, H. W. (2015) Mohawk promotes the tenogenesis of mesenchymal stem cells through activation of the TGFbeta signaling pathway. *Stem Cells* **33**, 443-455
29. Ito, Y., Toriuchi, N., Yoshitaka, T., Ueno-Kudoh, H., Sato, T., Yokoyama, S., Nishida, K., Akimoto, T., Takahashi, M., Miyaki, S., and Asahara, H. (2010) The Mohawk homeobox gene is a critical regulator of tendon differentiation. *Proc Natl Acad Sci U S A* **107**, 10538-10542
30. Docheva, D., Hunziker, E. B., Fassler, R., and Brandau, O. (2005) Tenomodulin is necessary for tenocyte proliferation and tendon maturation. *Mol Cell Biol* **25**, 699-705
31. O'Brien, M. (1997) Structure and metabolism of tendons. *Scand J Med Sci Sports* **7**, 55-61
32. Saneyasu, T., Yoshioka, S., and Sakai, T. (2016) Mechanisms of Collagen Network Organization in Response to Tissue/Organ Damage. in *Composition and Function of the Extracellular Matrix in the Human Body*. pp
33. Moriya, K., Bae, E., Honda, K., Sakai, K., Sakaguchi, T., Tsujimoto, I., Kamisoyama, H., Keene, D. R., Sasaki, T., and Sakai, T. (2011) A fibronectin-independent mechanism of collagen fibrillogenesis in adult liver remodeling. *Gastroenterology* **140**, 1653-1663
34. Hynes, R. O. (1992) Integrins: versatility, modulation, and signaling in cell adhesion. *Cell* **69**, 11-25
35. Hynes, R. O. (2002) Integrins: bidirectional, allosteric signaling machines. *Cell* **110**, 673-687
36. Giancotti, F. G., and Ruoslahti, E. (1999) Integrin signaling. *Science* **285**, 1028-1032
37. Schwartz, M. A., and Ginsberg, M. H. (2002) Networks and crosstalk: integrin signalling spreads. *Nat Cell Biol* **4**, E65-68
38. Hughes, P. E., and Pfaff, M. (1998) Integrin affinity modulation. *Trends Cell Biol* **8**, 359-364
39. Lauffenburger, D. A., and Horwitz, A. F. (1996) Cell migration: a physically integrated molecular process. *Cell* **84**, 359-369
40. Ridley, A. J., Schwartz, M. A., Burridge, K., Firtel, R. A., Ginsberg, M. H., Borisy, G., Parsons, J. T., and Horwitz, A. R. (2003) Cell migration: integrating signals from front to back. *Science* **302**, 1704-1709

41. DeMali, K. A., Wennerberg, K., and Burridge, K. (2003) Integrin signaling to the actin cytoskeleton. *Curr Opin Cell Biol* **15**, 572-582
42. Hall, A. (1998) Rho GTPases and the actin cytoskeleton. *Science* **279**, 509-514
43. Galbraith, C. G., Yamada, K. M., and Galbraith, J. A. (2007) Polymerizing actin fibers position integrins primed to probe for adhesion sites. *Science* **315**, 992-995
44. Krause, M., and Gautreau, A. (2014) Steering cell migration: lamellipodium dynamics and the regulation of directional persistence. *Nature reviews. Molecular cell biology* **15**, 577-590
45. Petrie, R. J., Doyle, A. D., and Yamada, K. M. (2009) Random versus directionally persistent cell migration. *Nature reviews. Molecular cell biology* **10**, 538-549
46. Maeda, T., Sakabe, T., Sunaga, A., Sakai, K., Rivera, A. L., Keene, D. R., Sasaki, T., Stavnezer, E., Iannotti, J., Schweitzer, R., Ilic, D., Baskaran, H., and Sakai, T. (2011) Conversion of mechanical force into TGF-beta-mediated biochemical signals. *Curr Biol* **21**, 933-941
47. Postlethwaite, A. E., and Kang, A. H. (1976) Collagen-and collagen peptide-induced chemotaxis of human blood monocytes. *J Exp Med* **143**, 1299-1307
48. Postlethwaite, A. E., Seyer, J. M., and Kang, A. H. (1978) Chemotactic attraction of human fibroblasts to type I, II, and III collagens and collagen-derived peptides. *Proc Natl Acad Sci U S A* **75**, 871-875
49. Iwai, K., Hasegawa, T., Taguchi, Y., Morimatsu, F., Sato, K., Nakamura, Y., Higashi, A., Kido, Y., Nakabo, Y., and Ohtsuki, K. (2005) Identification of food-derived collagen peptides in human blood after oral ingestion of gelatin hydrolysates. *Journal of agricultural and food chemistry* **53**, 6531-6536
50. Taga, Y., Kusubata, M., Ogawa-Goto, K., and Hattori, S. (2014) Highly accurate quantification of hydroxyproline-containing peptides in blood using a protease digest of stable isotope-labeled collagen. *Journal of agricultural and food chemistry* **62**, 12096-12102
51. Liu, Z., Wang, C., Liu, Q., Meng, Q., Cang, J., Mei, L., Kaku, T., and Liu, K. (2011) Uptake, transport and regulation of JBP485 by PEPT1 in vitro and in vivo. *Peptides* **32**, 747-754
52. Gallo, M., Defaus, S., and Andreu, D. (2019) 1988-2018: Thirty years of drug smuggling at the nano scale. Challenges and opportunities of cell-penetrating peptides in biomedical research. *Arch Biochem Biophys* **661**, 74-86
53. Durzyńska, J., Przysiecka, Ł., Nawrot, R., Barylski, J., Nowicki, G., Warowicka, A., Musidlak, O., and Goździcka-Józefiak, A. (2015) Viral and other cell-penetrating peptides as vectors of therapeutic agents in medicine. *The Journal of pharmacology and experimental therapeutics* **354**, 32-42
54. Tabujew, I., Lelle, M., and Peneva, K. J. B. (2015) Cell-penetrating peptides for nanomedicine–how to choose the right peptide. *BioNanoMaterials* **16**, 59-72
55. Huang, A. H., Lu, H. H., and Schweitzer, R. (2015) Molecular regulation of tendon cell fate during development. *J Orthop Res*
56. Iwasaki, A., Sakai, K., Moriya, K., Sasaki, T., Keene, D. R., Akhtar, R., Miyazono, T., Yasumura, S., Watanabe, M., Morishita, S., and Sakai, T. (2016) Molecular Mechanism Responsible for Fibronectin-controlled Alterations in Matrix Stiffness in Advanced Chronic Liver Fibrogenesis. *J Biol Chem* **291**, 72-88
57. Canty, E. G., and Kadler, K. E. (2005) Procollagen trafficking, processing and fibrillogenesis. *J Cell Sci* **118**, 1341-1353
58. Saneyasu, T., Yoshioka, S., and Sakai, T. (2016) Mechanisms of Collagen Network Organization in Response to Tissue/Organ Damage. *In: Composition and Function of the Extracellular Matrix in the Human Body*, pp235-260
59. Perez-Riverol, Y., Csordas, A., Bai, J., Bernal-Llinares, M., Hewapathirana, S., Kundu, D. J., Inuganti, A., Griss, J., Mayer, G., Eisenacher, M., Pérez, E., Uszkoreit, J., Pfeuffer, J., Sachsenberg, T., Yilmaz, S., Tiwary, S., Cox, J., Audain, E., Walzer, M., Jarnuczak, A. F., Ternent, T., Brazma, A., and Vizcaíno, J. A. (2019) The PRIDE database and related tools and resources in 2019: improving support for quantification data. *Nucleic Acids Res* **47**, D442-d450
60. Zhang, W., and Liu, H. T. (2002) MAPK signal pathways in the regulation of cell proliferation in mammalian cells. *Cell research* **12**, 9-18
61. Tanimura, S., and Takeda, K. (2017) ERK signalling as a regulator of cell motility. *Journal of biochemistry* **162**, 145-154

62. Laskin, D. L., Kimura, T., Sakakibara, S., Riley, D. J., and Berg, R. A. (1986) Chemotactic activity of collagen-like polypeptides for human peripheral blood neutrophils. *J Leukoc Biol* **39**, 255-266
63. Jain, P., Worthylake, R. A., and Alahari, S. K. (2012) Quantitative analysis of random migration of cells using time-lapse video microscopy. *Journal of visualized experiments : JoVE*, e3585
64. Truong, H., and Danen, E. H. (2009) Integrin switching modulates adhesion dynamics and cell migration. *Cell adhesion & migration* **3**, 179-181
65. Sakai, T., Zhang, Q., Fassler, R., and Mosher, D. F. (1998) Modulation of beta1A integrin functions by tyrosine residues in the beta1 cytoplasmic domain. *J Cell Biol* **141**, 527-538
66. Barkan, D., and Chambers, A. F. (2011) β1-integrin: a potential therapeutic target in the battle against cancer recurrence. *Clinical cancer research : an official journal of the American Association for Cancer Research* **17**, 7219-7223
67. Schunck, M., and Oesser, S. (2013) Specific collagen peptides benefit the biosynthesis of matrix molecules of tendons and ligaments. *Journal of the International Society of Sports Nutrition* **10**, P23
68. Nigam, S. K. (2015) What do drug transporters really do? *Nature reviews. Drug discovery* **14**, 29-44
69. Nakatani, S., Mano, H., Sampei, C., Shimizu, J., and Wada, M. (2009) Chondroprotective effect of the bioactive peptide prolyl-hydroxyproline in mouse articular cartilage in vitro and in vivo. *Osteoarthritis Cartilage* **17**, 1620-1627
70. Havis, E., Bonnin, M. A., Olivera-Martinez, I., Nazaret, N., Ruggiu, M., Weibel, J., Durand, C., Guerquin, M. J., Bonod-Bidaud, C., Ruggiero, F., Schweitzer, R., and Duprez, D. (2014) Transcriptomic analysis of mouse limb tendon cells during development. *Development* **141**, 3683-3696
71. Havis, E., Bonnin, M. A., Esteves de Lima, J., Charvet, B., Milet, C., and Duprez, D. (2016) TGFbeta and FGF promote tendon progenitor fate and act downstream of muscle contraction to regulate tendon differentiation during chick limb development. *Development* **143**, 3839-3851
72. Shukunami, C., Takimoto, A., Oro, M., and Hiraki, Y. (2006) Scleraxis positively regulates the expression of tenomodulin, a differentiation marker of tenocytes. *Dev Biol* **298**, 234-247
73. Mana, G., Valdembri, D., and Serini, G. (2020) Conformationally active integrin endocytosis and traffic: why, where, when and how? *Biochemical Society transactions* **48**, 83-93
74. Moreno-Layseca, P., Icha, J., Hamidi, H., and Ivaska, J. (2019) Integrin trafficking in cells and tissues. *Nat Cell Biol* **21**, 122-132
75. Pozzi, A., Wary, K. K., Giancotti, F. G., and Gardner, H. A. (1998) Integrin alpha1beta1 mediates a unique collagen-dependent proliferation pathway in vivo. *The Journal of cell biology* **142**, 587-594
76. Sastry, S. K., Lakonishok, M., Wu, S., Truong, T. Q., Huttenlocher, A., Turner, C. E., and Horwitz, A. F. (1999) Quantitative changes in integrin and focal adhesion signaling regulate myoblast cell cycle withdrawal. *J Cell Biol* **144**, 1295-1309
77. Manohar, A., Shome, S. G., Lamar, J., Stirling, L., Iyer, V., Pumiglia, K., and DiPersio, C. M. (2004) Alpha 3 beta 1 integrin promotes keratinocyte cell survival through activation of a MEK/ERK signaling pathway. *J Cell Sci* **117**, 4043-4054
78. Vicente-Manzanares, M., and Horwitz, A. R. (2011) Adhesion dynamics at a glance. *J Cell Sci* **124**, 3923-3927
79. Vicente-Manzanares, M., Choi, C. K., and Horwitz, A. R. (2009) Integrins in cell migration--the actin connection. *J Cell Sci* **122**, 199-206
80. Innocenti, M. (2018) New insights into the formation and the function of lamellipodia and ruffles in mesenchymal cell migration. *Cell adhesion & migration* **12**, 401-416
81. Sharma, P., and Maffulli, N. (2006) Biology of tendon injury: healing, modeling and remodeling. *J Musculoskelet Neuronal Interact* **6**, 181-190
82. Sakabe, T., and Sakai, T. (2011) Musculoskeletal diseases--tendon. *Br Med Bull* **99**, 211-225
83. Aslan, H., Kimelman-Bleich, N., Pelled, G., and Gazit, D. (2008) Molecular targets for tendon neoformation. *J Clin Invest* **118**, 439-444

84. Kusubata, M., Koyama, Y., Tometsuka, C., Shigemura, Y., and Sato, K. (2015) Detection of endogenous and food-derived collagen dipeptide prolylhydroxyproline (Pro-Hyp) in allergic contact dermatitis-affected mouse ear. *Biosci Biotechnol Biochem* **79**, 1356-1361
85. Jimi, S., Sato, K., Kimura, M., Suzumiya, J., Hara, S., De Francesco, F., and Ohjimi, H. (2017) G-CSF administration accelerates cutaneous wound healing accompanied with increased Pro-Hyp production in db/db mice. *Clin. Res. Dermatol* **4**, 1-9
86. Ueda, H., Meguri, N., Minaguchi, J., Watanabe, T., Nagayasu, A., Hosaka, Y., Tangkawattana, P., Kokai, Y., and Takehana, K. (2008) Effect of collagen oligopeptide injection on rabbit tenositis. *J Vet Med Sci* **70**, 1295-1300
87. Praet, S. F. E., Purdam, C. R., Welvaert, M., Vlahovich, N., Lovell, G., Burke, L. M., Gaida, J. E., Manzanero, S., Hughes, D., and Waddington, G. (2019) Oral Supplementation of Specific Collagen Peptides Combined with Calf-Strengthening Exercises Enhances Function and Reduces Pain in Achilles Tendinopathy Patients. *Nutrients* **11**
88. Taga, Y., Iwasaki, Y., Shigemura, Y., and Mizuno, K. (2019) Improved in Vivo Tracking of Orally Administered Collagen Hydrolysate Using Stable Isotope Labeling and LC-MS Techniques. *Journal of agricultural and food chemistry* **67**, 4671-4678
89. Wang, W., Wang, F., Lu, F., Xu, S., Hu, W., Huang, J., Gu, Q., and Sun, X. (2011) The antiangiogenic effects of integrin alpha5beta1 inhibitor (ATN-161) in vitro and in vivo. *Invest Ophthalmol Vis Sci* **52**, 7213-7220
90. Sakai, T., Li, S., Docheva, D., Grashoff, C., Sakai, K., Kostka, G., Braun, A., Pfeifer, A., Yurchenco, P. D., and Fassler, R. (2003) Integrin-linked kinase (ILK) is required for polarizing the epiblast, cell adhesion, and controlling actin accumulation. *Genes Dev* **17**, 926-940
91. Honda, K., Sakaguchi, T., Sakai, K., Schmedt, C., Ramirez, A., Jorcano, J. L., Tarakhovsky, A., Kamisoyama, H., and Sakai, T. (2007) Epidermal hyperplasia and papillomatosis in mice with a keratinocyte-restricted deletion of csk. *Carcinogenesis* **28**, 2074-2081
92. Ogese, M. O., Jenkins, R. E., Adair, K., Tailor, A., Meng, X., Faulkner, L., Enyindah, B. O., Schofield, A., Diaz-Nieto, R., Ressel, L., Eagle, G. L., Kitteringham, N. R., Goldring, C. E., Park, B. K., Naisbitt, D. J., and Betts, C. (2019) Exosomal Transport of Hepatocyte-Derived Drug-Modified Proteins to the Immune System. *Hepatology (Baltimore, Md.)* **70**, 1732-1749
93. Huang da, W., Sherman, B. T., and Lempicki, R. A. (2009) Systematic and integrative analysis of large gene lists using DAVID bioinformatics resources. *Nature protocols* **4**, 44-57
94. Huang da, W., Sherman, B. T., and Lempicki, R. A. (2009) Bioinformatics enrichment tools: paths toward the comprehensive functional analysis of large gene lists. *Nucleic Acids Res* **37**, 1-13
95. Sakai, T., Peyruchaud, O., Fassler, R., and Mosher, D. F. (1998) Restoration of beta1A integrins is required for lysophosphatidic acid-induced migration of beta1-null mouse fibroblastic cells. *J Biol Chem* **273**, 19378-19382
96. Gorelik, R., and Gautreau, A. (2014) Quantitative and unbiased analysis of directional persistence in cell migration. *Nature protocols* **9**, 1931-1943

Figure Legends

Fig. 1. Cell response to Pro-Hyp in adult tenocytes and tendon progenitor cells.
(A) Dose-responses to Pro-Hyp peptide. Cells were cultured with different concentrations of Pro-Hyp for 24 hrs. Dose responses are shown relative to the control value of 100% (cultured without Pro-Hyp). Error bars represent the standard deviation (n = 3).
(B) Cell proliferation activity. Cells were cultured with 200 or 500 µg/mL Pro-Hyp for up to 3 days. Error bars represent the standard deviation (n = 3). **, P < 0.01; ***, P < 0.001: significantly different compared to untreated controls in post-hoc analysis.

Fig. 2. Uptake of Pro-Hyp into adult tenocytes.
(A) Time-course of uptake of stable isotopically labeled Pro-Hyp (SI-Pro-Hyp; 200 µg/mL) at 37 °C in adult tenocytes. Error bars represent the standard deviation (n = 4).
(B) Accumulation of SI-Pro-Hyp in tenocytes after 60 min at 37°C and 4 °C. Error bars represent the standard deviation (n = 4). **, P < 0.01.
(C) Subcellular localization analysis of 200 µg/mL SI-Pro-Hyp in adult tenocytes after 60 min at 37°C. Error bars represent the standard deviation (n = 4).

Fig. 3. Enhanced tenogenic differentiation in response to Pro-Hyp in adult tenocytes and tendon progenitor cells.
(A) Real-time PCR analysis of *Scx*, *Sox 9*, *Mkx*, and *Tnmd* mRNA levels. Cells were treated with Pro-Hyp and cultured for 3, 6 and 11 days. mRNA expression levels are shown relative to the control value of 1 (untreated cells). Error bars represent the standard deviation (n = 3). *, P < 0.05; **, P < 0.01; ***, P < 0.001 (in post-hoc analysis).
(B) The effect of Pro-Hyp on ScxGFP expression in adult tenocytes and tendon progenitor cells. In adult tenocyte cultures, TGF-β1 (2 ng/mL) was used as a positive control (46). Scale bars, 100 µm.

Fig. 4. Upregulated ECM mRNA expression and protein production, and type I collagen network organization in tendon cells.
(A) Real-time PCR analysis of *type I collagen* (*Col1a1)*, *fibronectin*, and *type V collagen* (*Col5a1)* mRNA levels in tendon cells. Cells were cultured with Pro-Hyp for 3 days. mRNA expression levels are shown relative to the control value of 1 (untreated cells). Error bars represent the standard deviation (n = 3). *, P < 0.05 (in post-hoc analysis).
(B) Western blot analysis of type I collagen (COL1A1) and fibronectin in cellular lysates of tendon cells. Cells were cultured with Pro-Hyp for 3 days. Band intensity was measured by densitometry and normalized to α-tubulin (loading control). α-tubulin blots were reused in each analysis. The type I collagen and fibronectin levels are shown relative to the control value of 1 (untreated cells). Error bars represent the standard deviation (n = 3). *, P < 0.05 (in post-hoc analysis).

(C) Enhanced type I collagen network organization in adult tenocytes. (**Upper panels**) Phase-contrast micrographs and immunofluorescence staining for type I collagen (red)/ DAPI (blue) with Pro-Hyp for 3 days. Scale bars, 100 μm. (**Lower panel**) Quantification of type I collagen positivity by densitometric analysis. Error bars represent the standard deviation (n = 3). *, P < 0.05 (in post-hoc analysis).

Fig. 5. Effect of Pro-Hyp on phospho-ERK (ERK[p202/204]) expression and cell migration activity in adult tenocytes and tendon progenitor cells.

(A) Western blot analysis of phospho-ERK and total ERK (left panels), and analysis of phospho-ERK intensities (right panels). Band intensity was measured by densitometry and normalized to total ERK. Each phospho-ERK level is shown relative to the control value of 1 (at time 0 of untreated cells). Error bars represent the standard deviation (n = 3). MW, molecular weight marker. *, P < 0.05 (in post-hoc analysis).

(B) Cell migration of tendon cells through gelatin-coated filters using Boyden chamber. Pro-Hyp (200 or 500 μg/mL) was added in the lower chamber. Bars represent the mean cell number/0.785 mm^2 field. Error bars represent the standard deviation (n = 4). PDGF (10 ng/mL) was used as a positive control. **, P < 0.01; ***, P < 0.001 (in post-hoc analysis).

Fig. 6. Effect of Pro-Hyp on cell displacement and velocity in adult tenocytes.

(A) (**Upper panels**) Time-lapse images at 4 hr (the time point when Pro-Hyp was added) and 15 hr in adult tenocytes. In “Control”, cells were analyzed for 15 hr-observation periods without Pro-Hyp. Red arrows indicate lamellipodia-like protrusions. Scale bars, 100 μm. (**Lower panel**) Percentage of cells showing lamellipodial protrusions for 11 hr-observation periods. Error bars represent the standard deviation. ***, P < 0.001 (in post-hoc analysis).

(B) Trajectory plots measured by cell displacement with Pro-Hyp in adult tenocytes for 11 hrs. The X- and Y-axes show cell movement observed every 10 min for 11 hrs.

(C) (**Left panel**) Percentage of cells showing directional movement with Pro-Hyp (cells that migrate with a directionality ratio of more than 0.8; see details in Materials and methods). (**Middle and right panels**) Percentage of cells moving more than 10 μm (**Middle panel**) and more than 5 μm/hr (**Right panel)** for 11-hr observation periods. Error bars represent the standard deviation. **, P < 0.01; ***, P < 0.001 (in post-hoc analysis).

Fig. 7. Engagement of β1-integrin- and ERK-signaling in Pro-Hyp-mediated cell migration.

(A) (**Left panels**) Immunofluorescence staining for β1-integrin (clone 9EG7, which recognizes an extracellular epitope of ligand-inducible active β1 (65): green)/DAPI (blue) and F-actin (red)/DAPI (blue). Adult tenocytes were treated with 500 μg/mL Pro-Hyp for 6 hrs. Scale bars, 20 μm. (**Right panels**) The numbers of active β1-integrin-containing focal contacts, and the thickness of F-actin filaments when cells were treated with 500 μg/mL Pro-Hyp for 6 hrs. Error bars represent the standard deviation (n = 4; 4-spearate culture experiments). **, P < 0.01; ***, P < 0.001.

(B) Effect of MEK1/2 inhibitor PD98059 or α5β1-integrin antagonist ATN-161 on Pro-Hyp-mediated cell migration in adult tenocytes using Boyden chamber. Cell migration activity is shown relative to the control value of 100% (cells treated with 200 µg/mL Pro-Hyp). Error bars represent the standard deviation (n = 5). ***, $P < 0.001$ (in post-hoc analysis).

(C) Effect of ATN-161 on uptake of stable isotopically labeled Pro-Hyp (SI-Pro-Hyp; 200 µg/mL) in adult tenocytes for 60 min at 37°C. Error bars represent the standard deviation (n = 8). ***, $P < 0.001$.

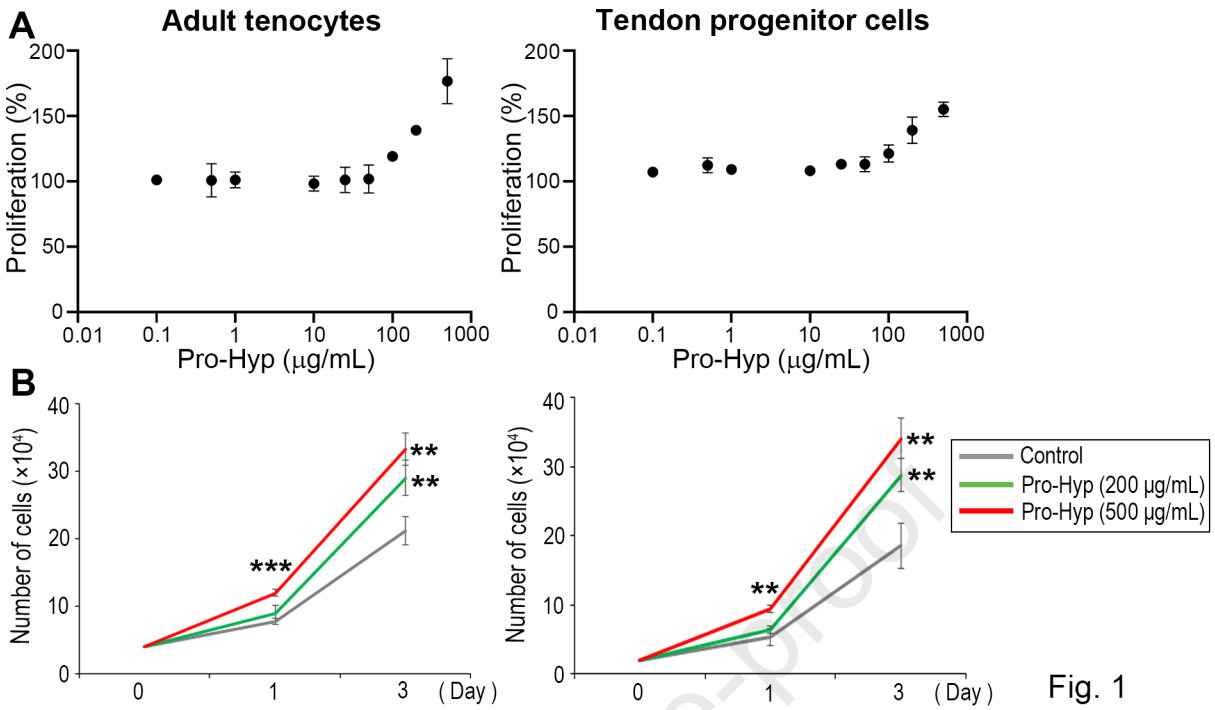

Fig. 1

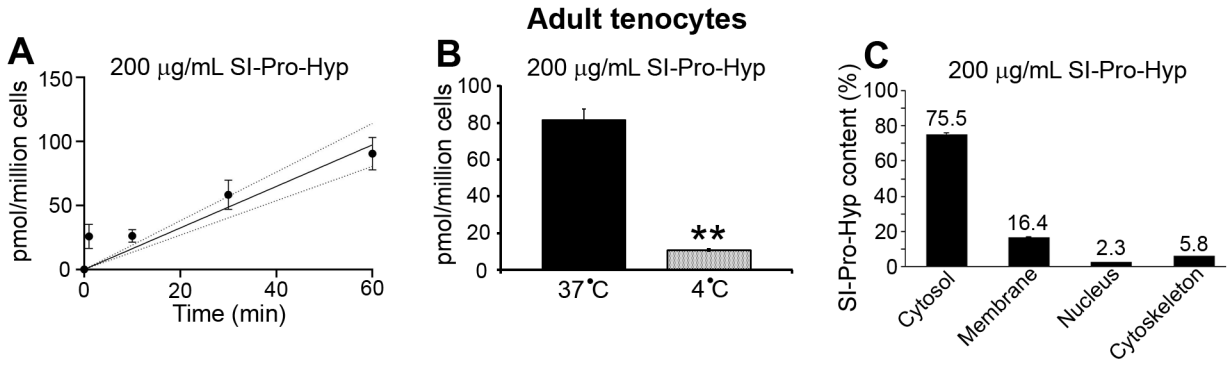

Fig. 2

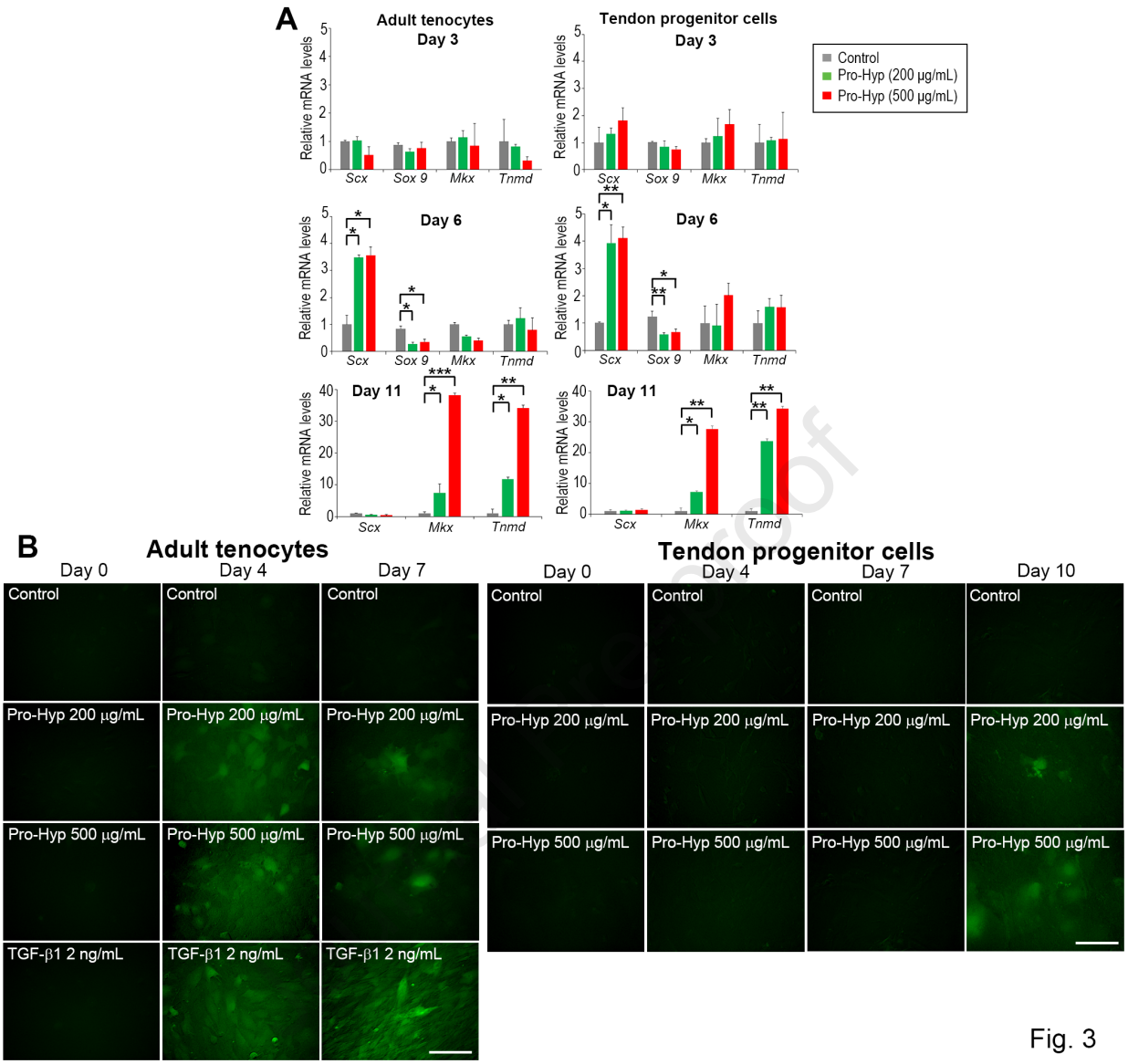
A
Adult tenocytes
Tendon progenitor cells
Day 3
Day 6
Day 11
Relative mRNA levels
Scx
Sox 9
Mkx
Tnmd
Control
Pro-Hyp (200 μg/mL)
Pro-Hyp (500 μg/mL)
B
Adult tenocytes
Tendon progenitor cells
Day 0
Day 4
Day 7
Day 10
Control
Pro-Hyp 200 μg/mL
Pro-Hyp 500 μg/mL
TGF-β1 2 ng/mL

Fig. 3

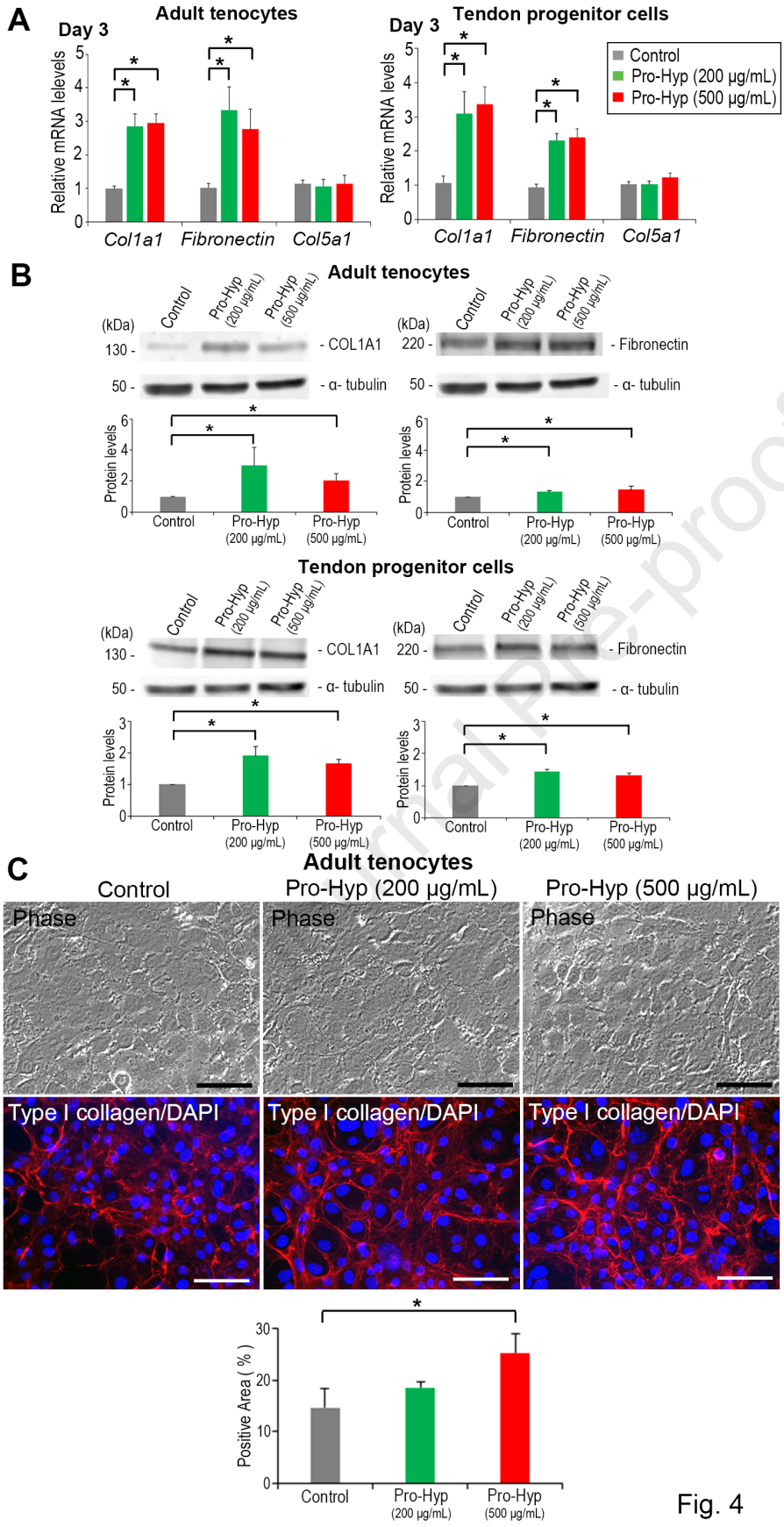
A
Adult tenocytes
Day 3
Relative mRNA levels
Col1a1
Fibronectin
Col5a1
Tendon progenitor cells
Control
Pro-Hyp (200 μg/mL)
Pro-Hyp (500 μg/mL)
B
Adult tenocytes
(kDa)
130 -
- COL1A1
50 -
- α- tubulin
220 -
- Fibronectin
Protein levels
Tendon progenitor cells
C
Adult tenocytes
Control
Pro-Hyp (200 μg/mL)
Pro-Hyp (500 μg/mL)
Phase
Type I collagen/DAPI
Positive Area (%)

Fig. 4

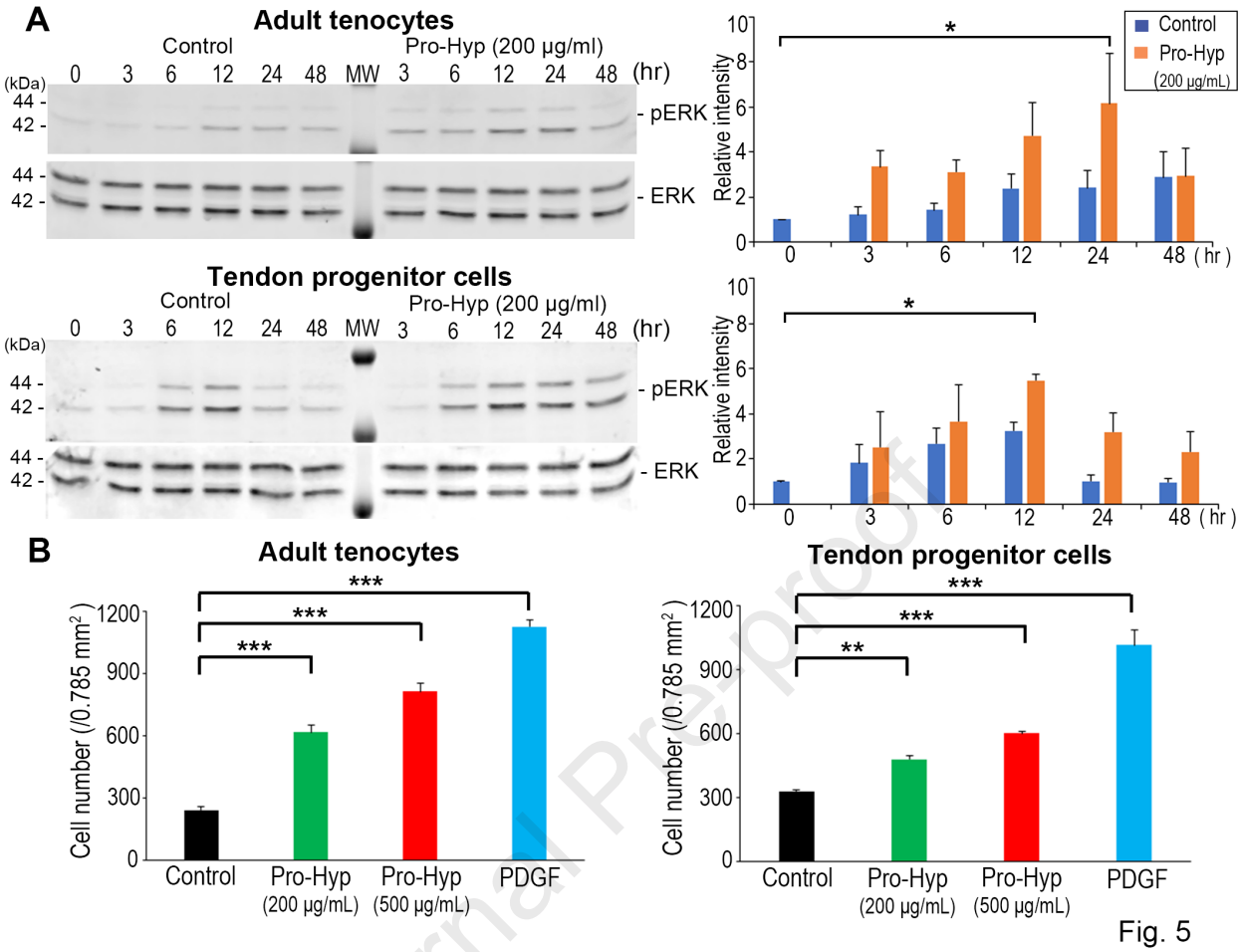

Fig. 5

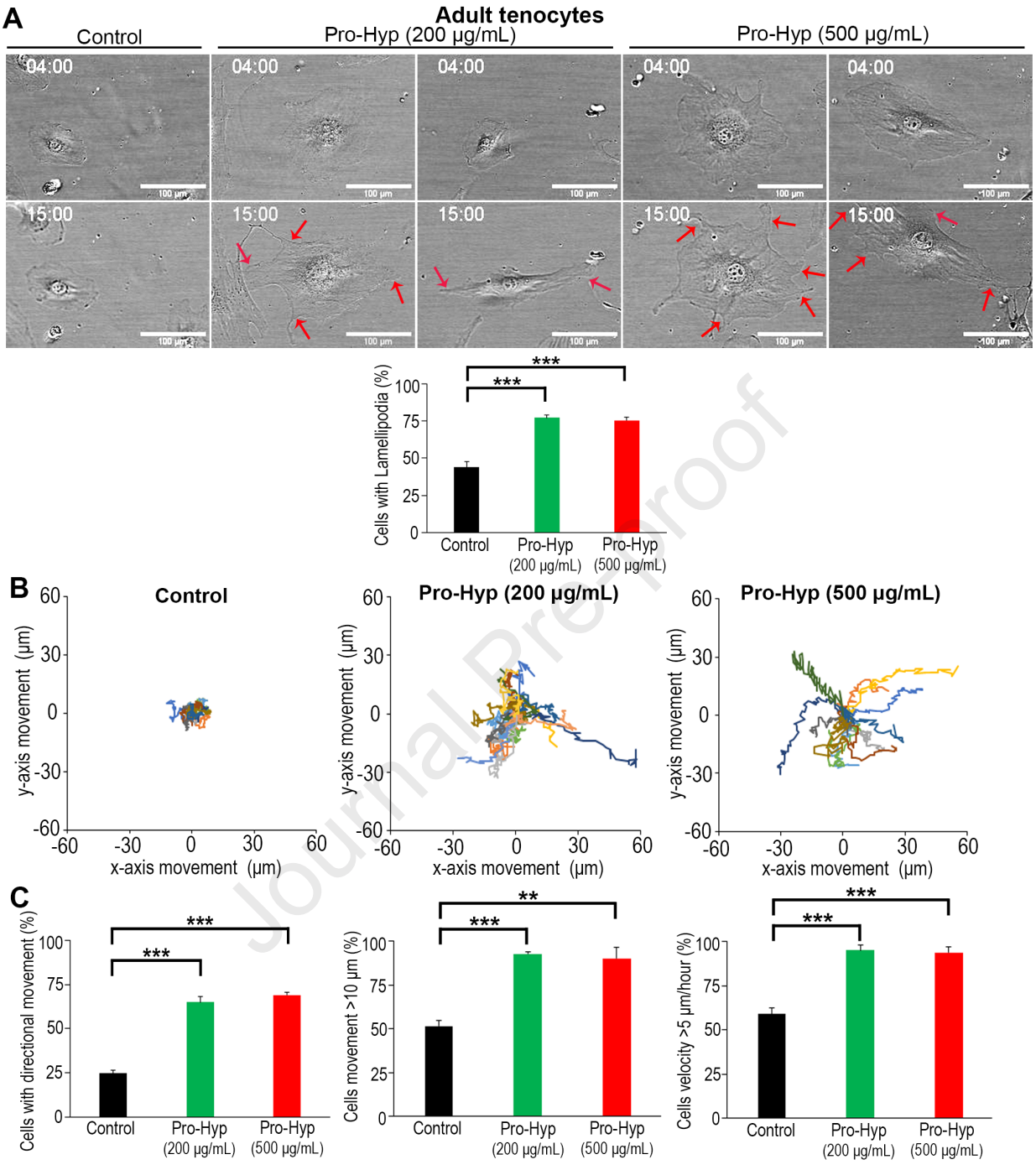

Fig. 6

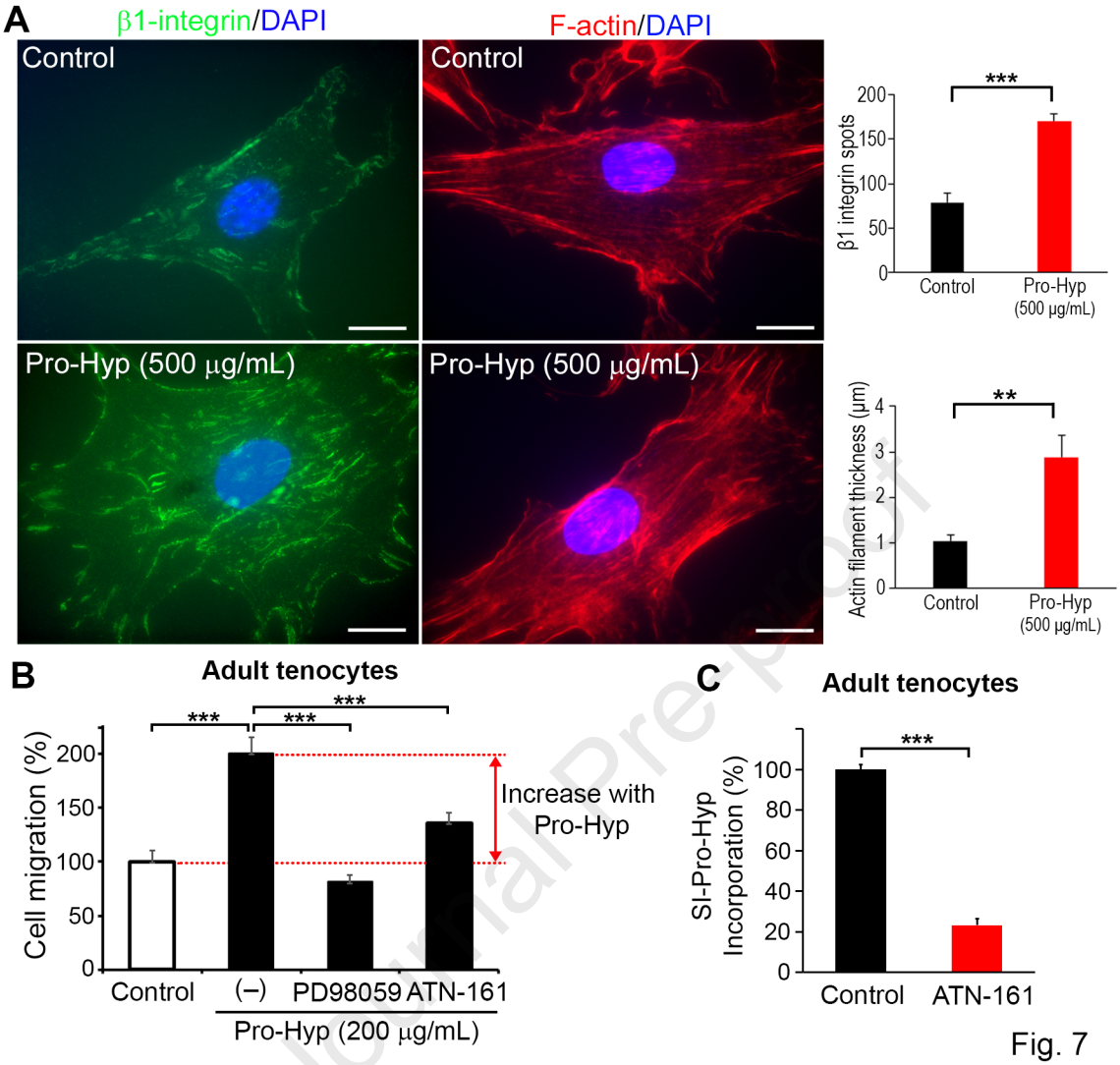

Fig. 7

Supporting Information

The dipeptide prolyl-hydroxyproline promotes cellular homeostasis and lamellipodia-driven motility via active β1-integrin in adult tendon cells

Kentaro Ide, Sanai Takahashi, Keiko Sakai, Yuki Taga, Tomonori Ueno, David Dickens, Rosalind Jenkins, Francesco Falciani, Takako Sasaki, Kazuhiro Ooi, Shuichi Kawashiri, Kazunori Mizuno, Shunji Hattori, and Takao Sakai

Supplementary Figures and Legends

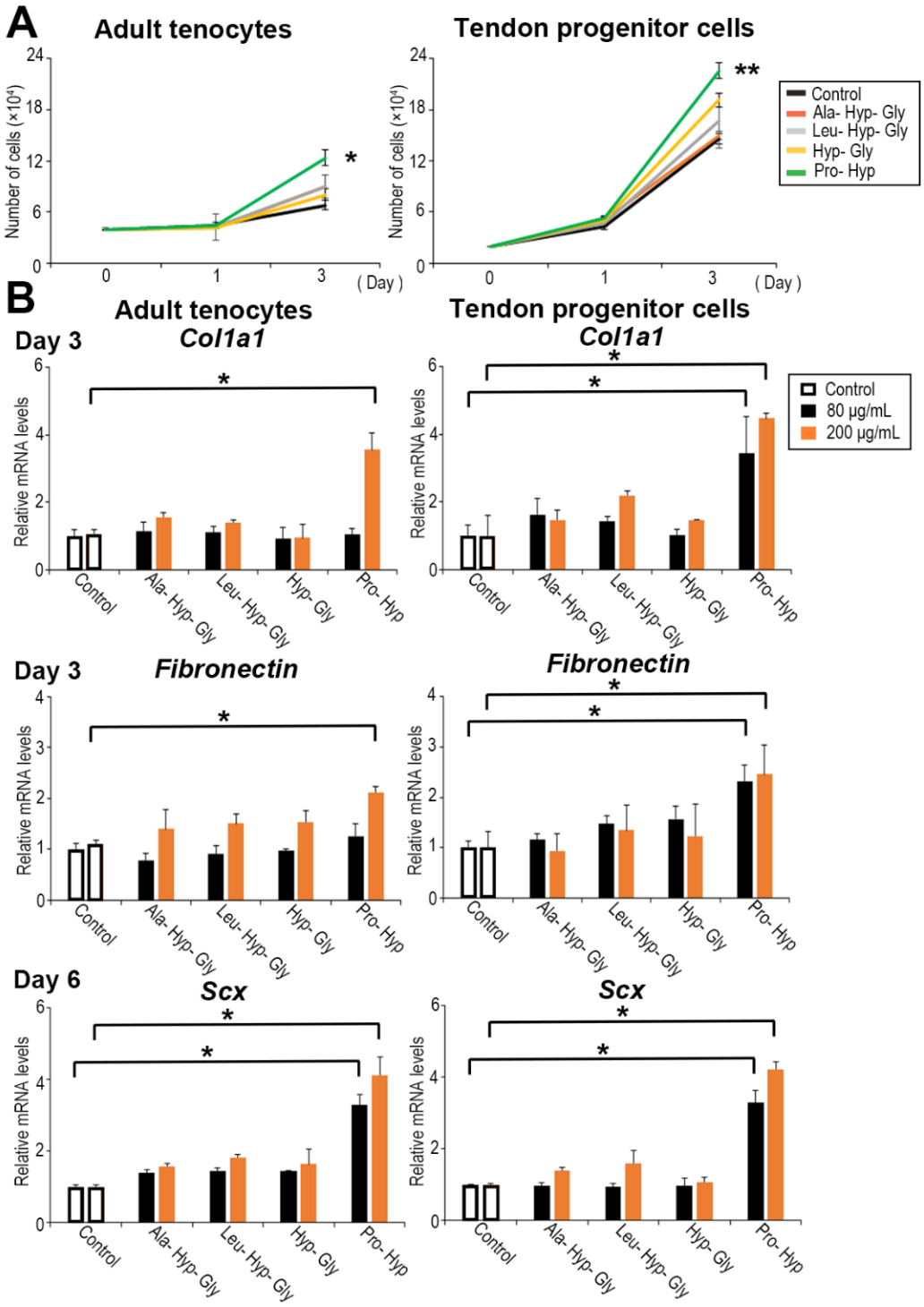

Suppl. Fig. 1. Physiological activity of Hyp-containing peptides in tendon cells.
(A) Cell proliferation assays. Adult tenocytes and tendon progenitor cells were cultured with 80 μg/mL of the Hyp-containing peptides Ala-Hyp-Gly, Leu-Hyp-Gly, Hyp-Gly, and Pro-Hyp, for up to 3 days.
(B) Real-time PCR analysis of *type I collagen* (*Col1a1)* and *fibronectin* (at day 3) and *Scx* (at day 6) mRNA levels. Cells were treated with 80 or 200 μg/mL of Hyp-containing peptides. Error bars represent the standard deviation (n = 3). *, $P < 0.05$; **, $P < 0.01$; ***, $P < 0.001$: significantly different compared to untreated controls (in post-hoc analysis).

Network No.	Score	Focus Molecules	Top Diseases and Functions
1	65	30	[Molecular Transport, Protein Trafficking, RNA Post-Transcriptional Modification]
2	51	25	[Cell Morphology, Organismal Injury and Abnormalities, Skeletal and Muscular Disorders]
3	45	23	[Cellular Assembly and Organization, Molecular Transport, RNA Trafficking]
4	37	20	[Cellular Movement, Embryonic Development, Renal and Urological System Development and Function]
5	26	15	[Cell Signaling, Cellular Assembly and Organization, Cellular Function and Maintenance]
6	21	13	[Cell Morphology, Cellular Assembly and Organization, DNA Replication, Recombination, and Repair]
7	21	13	[Cellular Development, Cellular Movement, Reproductive System Development and Function]
8	19	12	[Cancer, Post-Translational Modification, Protein Folding]

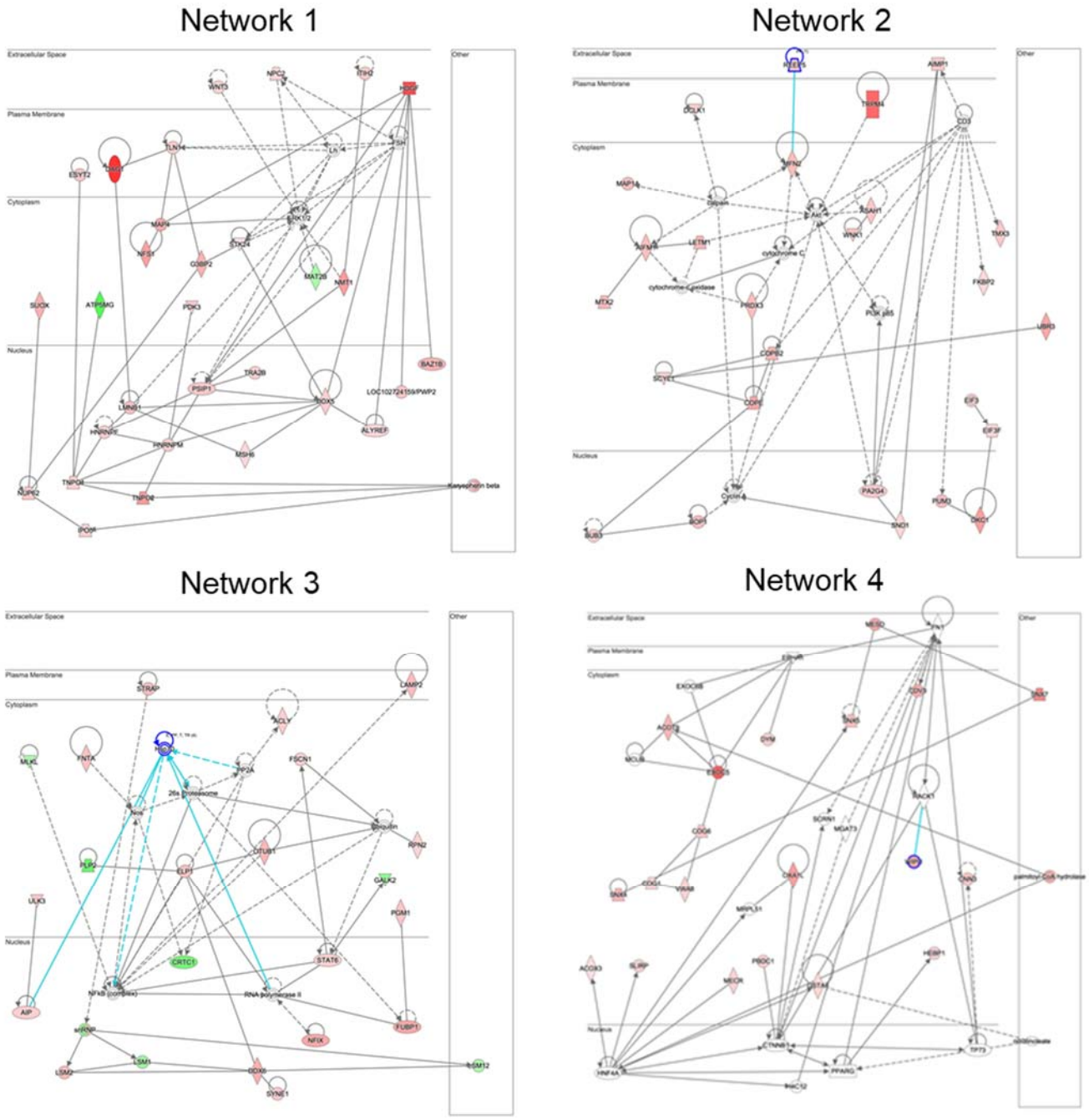

Suppl. Fig. 2. Proteomics analysis in adult tenocytes.
(**Upper panel**) The 8 networks that Ingenuity Pathway Analysis (IPA) identified linking the proteins differentially regulated at 6 hrs after Pro-Hyp treatment. Columns show the network ID, score, number of proteins included in each network and functions enriched in each network. (**Lower panels**) The 4 significant IPA networks identified using the list of proteins differentially regulated at 6 hrs after Pro-Hyp treatment. The network number represents each network described in the upper panel.

Suppl. Fig. 3. Live-cell imaging: Time-lapse microscopic analysis of adult tenocytes for 15 hrs. Adult tenocytes were (**A**) left untreated for 15 hrs or treated with (**B, C**) 200 µg/mL or (**D, E**) 500 µg/mL Pro-Hyp at the 4-hr time point and further observed for 11 hrs (total 15 hrs). The data are shown in separate video files (.avi). Scale bar, 100 µm.

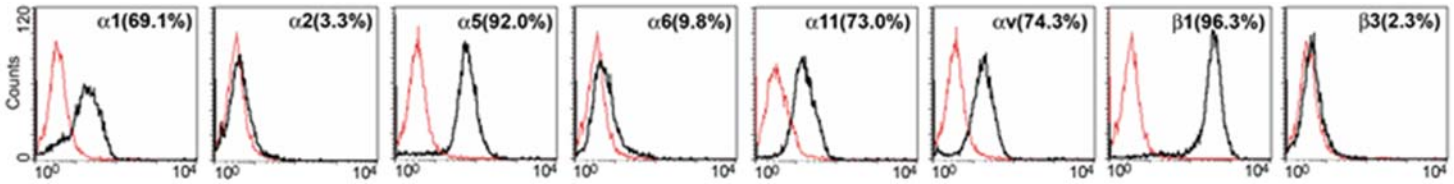

Suppl. Fig. 4. Integrin expression profiles in adult mouse primary tenocytes by FACS analysis. Adult mouse primary cultured tenocytes were stained with the anti-integrin antibodies α1 (clone Ha31/8), α2 (clone Ha1/29), α5 (clone 5H10-27), α6 (clone GoH3), α11, αv (clone RMV-7), β1 (clone Ha2/5), or β3 (clone 2C9.G2). Red and black histograms denote control fluorescence and cell/antibody-bound fluorescence, respectively. The percentage of positive cells is indicated in each panel.

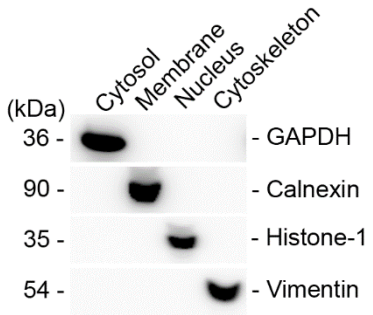

Suppl. Fig. 5. Western blot analysis of GAPDH (cytosolic marker), Calnexin (membrane), Histone-1 (nucleus), and Vimentin (cytoskeleton) after fractionation of cytosol, membrane/organelle, nucleus, and cytoskeleton from adult tenocytes.

Suppl. Table 1. Results of the ANOVA analyses

Figure	Statistics	ANOVA, F value	ANOVA, P value
Fig. 1B	Adult tenocytes, day 1	22.89	0.001
	Adult tenocytes, day 3	24.41	0.001
	Progenitors, day 1	20.8	0.002
	Progenitors, day 3	22.07	0.001
Fig. 3A	Adult tenocyts, day 6, Scx	43.02	< 0.001
	Adult tenocytes, day 6, Sox 9	13.17	0.002
	Progenitors, day 6, Scx	7.35	0.005
	Progenitors, day 6, Sox 9	6.8	0.008
	Adult tenocytes, day 11, Mkt	19.23	0.002
	Adult tenocytes, day 11, Tnmd	33.79	< 0.001
	Progenitors, day 11, Mkt	18.77	0.002
	Progenitors, day 11, Tnmd	20.95	0.001
Fig. 4A	Adult tenocytes, Col1a1	5.25	0.012
	Adult tenocytes, Fibronectin	4.43	0.025
	Progenitors, Col1a1	6.19	0.02
	Progenitors, Fibronectin	6.727	0.029
Fig. 4B	Adult tenocytes, COL1A1	5.8	0.019
	Adult tenocytes, Fibronectin	5.61	0.026
	Progenitors, COL1A1	6.81	0.007
	Progenitors, Fibronectin	15.62	0.001
Fig. 4C	Adult tenocytes, Col positive area	12.39	0.007
Fig. 5A#	Adult tenocytes, Control vs Pro-Hyp treated	8.39	0.008
	Adult tenocytes, Time course	2.62	0.05
	Adult tenocytes, Interaction	1.04	0.42
	Progenitors, Control vs Pro-Hyp treated	6.87	0.015
	Progenitors, Time course	4.26	0.007
	Progenitors, Interaction	0.56	0.73
Fig. 5B	Progenitors, Migration	66.42	< 0.001
Fig. 6A	Cells with lamellipodia	148.2	< 0.001
Fig. 6C	Directional movement	112.6	< 0.001
	Movement > 10 μm	13.09	< 0.001
	Velocity > 5 μm/hour	38.09	< 0.001
Fig. 7B	Cell migration	98.94	<0.001

Suppl. Fig. 1A	Adult tenocytes, day 3	5.38	0.014
	Progenitors, day 3	4.07	0.032
Suppl. Fig. 1B	Adult tenocytes, Col1a1 (200 μg/mL peptide)	12.67	< 0.001
	Progenitors, Col1a1 (80 μg/mL peptide)	4.05	0.033
	Progenitors, Col1A1 (200 mg/mL peptide)	8.95	0.006
	Adult tenocytes, Fibronectin (200 μg/mL peptide)	3.85	0.038
	Progenitors, Fibronectin (80 μg/mL peptide)	13.14	< 0.001
	Progenitors, Fibronectin (200 μg/mL peptide)	7	0.012
	Adult tenocytes, Scx (80 μg/mL peptide)	3.98	0.034
	Adult tenocytes, Scx (80 μg/mL peptide)	4.35	0.027
	Progenitors, Scx (80 μg/mL peptide)	4.95	0.018
	Progenitors, Scx (200 μg/mL peptide)	9.16	0.002

#, Data in Fig. 5A were analyzed using Two-way ANOVA.

Suppl. Table 2. Proteomics analysis in adult tenocytes. List of proteins where the fold change is significant for at least two time points by two-way ANOVA using the Database for Annotation, Visualization and Integrated Discovery (DAVID).

Protein	Accession	p-value	Ratio	Fold-Change	Fold-Change (Description)
Dystroglycan	Q62165	0.044	0.115	-8.681	6h + down vs 6h -
Mitochondrial import inner membrane translocase subunit Tim9	Q9WV98	0.049	0.118	-8.451	6h + down vs 6h -
ATP synthase subunit gamma, mitochondrial	Q91VR2	0.049	0.120	-8.358	6h + down vs 6h -
Hepatoma-derived growth factor	P51859	0.042	0.131	-7.647	6h + down vs 6h -
Exocyst complex component 5	Q3TPX4	0.027	0.148	-6.764	6h + down vs 6h -
RNA-binding protein Raly	Q64012	0.041	0.151	-6.641	6h + down vs 6h -
Transient receptor potential cation channel subfamily M member 4	Q7TN37	0.027	0.157	-6.360	6h + down vs 6h -
Protein virilizer homolog	A2AIV2	0.016	0.182	-5.500	6h + down vs 6h -
Myristoylated alanine-rich C-kinase substrate	P26645	0.018	0.190	-5.270	6h + down vs 6h -
Exocyst complex component 6B	A6H5Z3	0.033	0.192	-5.212	6h + down vs 6h -
Epidermal growth factor receptor kinase substrate 8-like protein 2	Q99K30	0.039	0.192	-5.198	6h + down vs 6h -
Sorting nexin-7	Q9CY18	0.026	0.196	-5.093	6h + down vs 6h -
Nucleoside diphosphate kinase B	Q01768	0.007	0.205	-4.885	6h + down vs 6h -
Cysteine and histidine-rich domain-containing protein 1	Q9D1P4	0.037	0.211	-4.739	6h + down vs 6h -
Endoribonuclease LACTB2	Q99KR3	0.035	0.213	-4.700	6h + down vs 6h -
Serine/threonine-protein kinase SIK3	Q6P4S6	0.047	0.214	-4.664	6h + down vs 6h -
NADH dehydrogenase [ubiquinone] 1 alpha subcomplex subunit 8	Q9DCJ5	0.041	0.218	-4.579	6h + down vs 6h -
60S ribosomal protein L35	Q6ZWV7	0.025	0.226	-4.427	6h + down vs 6h -
Beta-arrestin-1	Q8BWG8	0.033	0.228	-4.378	6h + down vs 6h -
Transportin-2	Q99LG2	0.003	0.233	-4.297	6h + down vs 6h -
Protein Noxp20	Q9D281	0.012	0.234	-4.278	6h + down vs 6h -
Vesicle-associated membrane protein-associated protein A	Q9WV55	0.015	0.235	-4.258	6h + down vs 6h -
Parathymosin	Q9D0J8	0.030	0.237	-4.228	6h + down vs 6h -
Glycylpeptide N-tetradecanoyltransferase 1	O70310	0.038	0.239	-4.183	6h + down vs 6h -
Cleavage and polyadenylation specificity factor subunit 3	Q9QXK7	0.042	0.241	-4.149	6h + down vs 6h -
Cohesin subunit SA-2	O35638	0.034	0.242	-4.132	6h + down vs 6h -
5'-AMP-activated protein kinase subunit beta-1	Q9R078	0.029	0.246	-4.062	6h + down vs 6h -
Mitochondrial inner membrane protein OXA1L	Q8BGA9	0.043	0.247	-4.053	6h + down vs 6h -
H/ACA ribonucleoprotein complex subunit DKC1	Q9ESX5	0.037	0.248	-4.038	6h + down vs 6h -
Serine/threonine-protein phosphatase 2A 65 kDa regulatory subunit A alpha isoform	Q76MZ3	0.033	0.249	-4.013	6h + down vs 6h -
Cysteine desulfurase, mitochondrial	Q9Z1J3	0.040	0.250	-3.997	6h + down vs 6h -
Eukaryotic translation initiation factor 2 subunit 2	Q99L45	0.012	0.257	-3.896	6h + down vs 6h -
THUMP domain-containing protein 3	P97770	0.002	0.257	-3.893	6h + down vs 6h -
Constitutive coactivator of PPAR-gamma-like protein 2	Q8C3F2	0.039	0.257	-3.889	6h + down vs 6h -
S-formylglutathione hydrolase	Q9R0P3	0.021	0.263	-3.800	6h + down vs 6h -
X-ray repair cross-complementing protein 5	P27641	0.025	0.265	-3.780	6h + down vs 6h -
Far upstream element-binding protein 1	Q91WJ8	0.027	0.270	-3.709	6h + down vs 6h -
WD repeat domain phosphoinositide-interacting protein 1	Q8R3E3	0.025	0.270	-3.699	6h + down vs 6h -
Plasminogen activator inhibitor 1 RNA-binding protein	Q9CY58	0.023	0.271	-3.687	6h + down vs 6h -
Coatomer subunit epsilon	O89079	0.026	0.273	-3.668	6h + down vs 6h -
E3 ubiquitin-protein ligase UBR3	Q5U430	0.017	0.274	-3.647	6h + down vs 6h -
Nuclear factor 1 X-type	P70257	0.019	0.276	-3.628	6h + down vs 6h -
LRP chaperone MESD	Q9ERE7	0.028	0.276	-3.623	6h + down vs 6h -
Microtubule-associated protein 4	P27546	0.017	0.278	-3.599	6h + down vs 6h -
Histone-binding protein RBBP4	Q60972	0.046	0.280	-3.572	6h + down vs 6h -
Cytoskeleton-associated protein 5	A2AGT5	0.028	0.283	-3.528	6h + down vs 6h -
Anaphase-promoting complex subunit 1	P53995	0.028	0.284	-3.527	6h + down vs 6h -
Aldose reductase-related protein 2	P45377	0.022	0.285	-3.511	6h + down vs 6h -
COMM domain-containing protein 4	Q9CQ02	0.032	0.291	-3.439	6h + down vs 6h -
Cytochrome b-c1 complex subunit 7	Q9D855	0.036	0.294	-3.400	6h + down vs 6h -
Sulfite oxidase, mitochondrial	Q8R086	0.031	0.296	-3.378	6h + down vs 6h -
Protein CDV3	Q4VAA2	0.044	0.297	-3.364	6h + down vs 6h -
Ran-binding protein 3	Q9CT10	0.029	0.302	-3.315	6h + down vs 6h -
Probable ATP-dependent RNA helicase DDX6	P54823	0.019	0.304	-3.289	6h + down vs 6h -
N-alpha-acetyltransferase 35, NatC auxiliary subunit	Q6PHQ8	0.011	0.304	-3.287	6h + down vs 6h -
Dual specificity mitogen-activated protein kinase kinase 4	P47809	0.009	0.305	-3.277	6h + down vs 6h -
Rabankyrin-5	Q810B6	0.046	0.305	-3.274	6h + down vs 6h -
Tyrosine-protein kinase BAZ1B	Q9Z277	0.035	0.307	-3.255	6h + down vs 6h -

Ras GTPase-activating protein-binding protein 2	P97379	0.022	0.309	-3.241	6h + down vs 6h -
Dedicator of cytokinesis protein 7	Q8R1A4	0.045	0.309	-3.231	6h + down vs 6h -
Mitochondrial fission 1 protein	Q9CQ92	0.038	0.319	-3.138	6h + down vs 6h -
Torsin-1B	Q9ER41	0.037	0.320	-3.129	6h + down vs 6h -
Elongation factor Ts, mitochondrial	Q9CZR8	0.013	0.321	-3.120	6h + down vs 6h -
Phosphoacetylglucosamine mutase	Q9CYR6	0.028	0.321	-3.115	6h + down vs 6h -
D-aminoacyl-tRNA deacylase 2	Q8BHA3	0.038	0.321	-3.115	6h + down vs 6h -
Elongation factor G, mitochondrial	Q8K0D5	0.046	0.323	-3.099	6h + down vs 6h -
Elongation factor 1-delta	P57776	0.014	0.323	-3.097	6h + down vs 6h -
Acyl-coenzyme A thioesterase 9, mitochondrial	Q9R0X4	0.049	0.324	-3.090	6h + down vs 6h -
Sorting nexin-4	Q91YJ2	0.025	0.324	-3.084	6h + down vs 6h -
14-3-3 protein gamma	P61982	0.028	0.324	-3.082	6h + down vs 6h -
Ribosomal L1 domain-containing protein 1	Q8BVY0	0.014	0.325	-3.075	6h + down vs 6h -
Mth938 domain-containing protein	Q8R0P4	0.002	0.327	-3.062	6h + down vs 6h -
Zinc finger C2HC domain-containing protein 1A	Q8BJH1	0.018	0.329	-3.043	6h + down vs 6h -
Coatomer subunit beta'	O55029	0.019	0.329	-3.040	6h + down vs 6h -
Ubiquitin thioesterase OTUB1	Q7TQI3	0.027	0.332	-3.010	6h + down vs 6h -
Mitochondrial proton/calcium exchanger protein	Q9Z2I0	0.039	0.334	-2.993	6h + down vs 6h -
Methyltransferase-like 26	Q9DCS2	0.034	0.335	-2.986	6h + down vs 6h -
Thyroid hormone receptor-associated protein 3	Q569Z6	0.039	0.335	-2.985	6h + down vs 6h -
Metaxin-2	O88441	0.047	0.336	-2.980	6h + down vs 6h -
Ezrin	P26040	0.050	0.338	-2.960	6h + down vs 6h -
Cytosolic acyl coenzyme A thioester hydrolase	Q91V12	0.023	0.342	-2.925	6h + down vs 6h -
Host cell factor 1	Q61191	0.042	0.343	-2.920	6h + down vs 6h -
Caprin-1	Q60865	0.010	0.348	-2.876	6h + down vs 6h -
Eukaryotic translation initiation factor 5B	Q05D44	0.032	0.352	-2.845	6h + down vs 6h -
Serine-threonine kinase receptor-associated protein	Q9Z1Z2	0.004	0.354	-2.825	6h + down vs 6h -
U6 snRNA-associated Sm-like protein LSm2	O35900	0.014	0.356	-2.809	6h + down vs 6h -
Microtubule-associated protein 1A	Q9QYR6	0.025	0.357	-2.799	6h + down vs 6h -
Pumilio homolog 3	Q8BKS9	0.009	0.361	-2.772	6h + down vs 6h -
Anaphase-promoting complex subunit 2	Q8BZQ7	0.003	0.361	-2.770	6h + down vs 6h -
Ribosome biogenesis protein BOP1	P97452	0.030	0.361	-2.770	6h + down vs 6h -
Lysosome-associated membrane glycoprotein 2	P17047	0.035	0.362	-2.762	6h + down vs 6h -
Protein transport protein Sec16A	E9QAT4	0.031	0.364	-2.750	6h + down vs 6h -
Mitofusin-2	Q80U63	0.000	0.364	-2.745	6h + down vs 6h -
Hemoglobin subunit alpha	P01942	0.033	0.365	-2.741	6h + down vs 6h -
Lamin-B1	P14733	0.021	0.366	-2.733	6h + down vs 6h -
Aconitate hydratase, mitochondrial	Q99KI0	0.037	0.366	-2.730	6h + down vs 6h -
14-3-3 protein zeta/delta	P63101	0.009	0.366	-2.730	6h + down vs 6h -
Fumarate hydratase, mitochondrial	P97807	0.041	0.370	-2.706	6h + down vs 6h -
Apoptosis-inducing factor 1, mitochondrial	Q9Z0X1	0.031	0.371	-2.693	6h + down vs 6h -
Sorting nexin-5	Q9D8U8	0.037	0.372	-2.691	6h + down vs 6h -
Thioredoxin-dependent peroxide reductase, mitochondrial	P20108	0.043	0.372	-2.688	6h + down vs 6h -
Protein farnesyltransferase/ geranylgeranyltransferase type-1 subunit alpha	Q61239	0.038	0.374	-2.673	6h + down vs 6h -
Protein Niban	Q3UW53	0.004	0.374	-2.671	6h + down vs 6h -
Eukaryotic translation initiation factor 5	P59325	0.045	0.375	-2.670	6h + down vs 6h -
Elongator complex protein 1	Q7TT37	0.025	0.379	-2.641	6h + down vs 6h -
Ataxin-10	P28658	0.026	0.380	-2.630	6h + down vs 6h -
Structural maintenance of chromosomes flexible hinge domain-containing protein 1	Q6P5D8	0.018	0.382	-2.616	6h + down vs 6h -
Probable 2-oxoglutarate dehydrogenase E1 component DHKTD1, mitochondrial	A2ATU0	0.042	0.384	-2.605	6h + down vs 6h -
Protein PRRC2C	Q3TLH4	0.024	0.385	-2.600	6h + down vs 6h -
V-type proton ATPase subunit C 1	Q9Z1G3	0.034	0.386	-2.590	6h + down vs 6h -
Nucleotide exchange factor SIL1	Q9EPK6	0.022	0.386	-2.590	6h + down vs 6h -
Serine/threonine-protein phosphatase 4 regulatory subunit 2	Q0VGB7	0.011	0.386	-2.589	6h + down vs 6h -
14-3-3 protein beta/alpha	Q9CQV8	0.009	0.387	-2.587	6h + down vs 6h -
Neurolysin, mitochondrial	Q91YP2	0.002	0.390	-2.565	6h + down vs 6h -
Farnesyl pyrophosphate synthase	Q920E5	0.018	0.393	-2.541	6h + down vs 6h -
Anaphase-promoting complex subunit 5	Q8BTZ4	0.029	0.395	-2.534	6h + down vs 6h -
Receptor expression-enhancing protein 5	Q60870	0.019	0.396	-2.527	6h + down vs 6h -
Serine/threonine-protein kinase ULK3	Q3U3Q1	0.030	0.398	-2.510	6h + down vs 6h -
LIM domain and actin-binding protein 1	Q9ERG0	0.032	0.399	-2.505	6h + down vs 6h -
Adenosine deaminase	P03958	0.004	0.399	-2.504	6h + down vs 6h -
Segment polarity protein dishevelled homolog DVL-2	Q60838	0.042	0.401	-2.494	6h + down vs 6h -
Serine/threonine-protein kinase WNK1	P83741	0.013	0.402	-2.486	6h + down vs 6h -
Periodic tryptophan protein 2 homolog	Q8BU03	0.039	0.404	-2.473	6h + down vs 6h -

Conserved oligomeric Golgi complex subunit 6	Q8R3I3	0.030	0.405	-2.468	6h + down vs 6h -
Protein arginine N-methyltransferase 1	Q9JIF0	0.028	0.405	-2.467	6h + down vs 6h -
Apoptotic chromatin condensation inducer in the nucleus	Q9JIX8	0.024	0.408	-2.451	6h + down vs 6h -
Calponin-3	Q9DAW9	0.039	0.409	-2.444	6h + down vs 6h -
Catenin alpha-1	P26231	0.023	0.410	-2.438	6h + down vs 6h -
NAD(P) transhydrogenase, mitochondrial	Q61941	0.045	0.411	-2.435	6h + down vs 6h -
Beta-1,3-glucosyltransferase	Q8BHT6	0.047	0.411	-2.432	6h + down vs 6h -
Nuclear pore complex protein Nup155	Q99P88	0.033	0.412	-2.428	6h + down vs 6h -
Extended synaptotagmin-2	Q3TZZ7	0.038	0.416	-2.405	6h + down vs 6h -
Methylmalonyl-CoA mutase, mitochondrial	P16332	0.012	0.418	-2.393	6h + down vs 6h -
Phosphoglucomutase-1	Q9D0F9	0.016	0.418	-2.392	6h + down vs 6h -
40S ribosomal protein S27	Q6ZWU9	0.018	0.418	-2.392	6h + down vs 6h -
Basigin	P18572	0.016	0.422	-2.369	6h + down vs 6h -
COP9 signalosome complex subunit 5	O35864	0.044	0.422	-2.368	6h + down vs 6h -
Pleckstrin homology-like domain family B member 2	Q8K1N2	0.015	0.423	-2.365	6h + down vs 6h -
Interleukin enhancer-binding factor 2	Q9CXY6	0.021	0.423	-2.364	6h + down vs 6h -
Proliferation-associated protein 2G4	P50580	0.035	0.425	-2.352	6h + down vs 6h -
Acid ceramidase	Q9WV54	0.041	0.425	-2.351	6h + down vs 6h -
Trifunctional purine biosynthetic protein adenosine-3	Q64737	0.040	0.427	-2.342	6h + down vs 6h -
Septin-11	Q8C1B7	0.025	0.428	-2.334	6h + down vs 6h -
PC4 and SFRS1-interacting protein	Q99JF8	0.030	0.429	-2.331	6h + down vs 6h -
Alpha-galactosidase A	P51569	0.012	0.429	-2.329	6h + down vs 6h -
Nesprin-1	Q6ZWR6	0.026	0.430	-2.326	6h + down vs 6h -
Interleukin-6 receptor subunit beta	Q00560	0.038	0.433	-2.311	6h + down vs 6h -
Collagen alpha-1(V) chain	O88207	0.035	0.433	-2.309	6h + down vs 6h -
DNA-directed RNA polymerase II subunit RPB2	Q8CFI7	0.029	0.435	-2.300	6h + down vs 6h -
Actin-related protein 3	Q99JY9	0.038	0.435	-2.297	6h + down vs 6h -
Transcription elongation factor SPT5	O55201	0.049	0.436	-2.293	6h + down vs 6h -
Major vault protein	Q9EQK5	0.029	0.438	-2.284	6h + down vs 6h -
Aminoacyl tRNA synthase complex-interacting multifunctional protein 1	P31230	0.049	0.439	-2.278	6h + down vs 6h -
Sorting nexin-12	O70493	0.033	0.440	-2.273	6h + down vs 6h -
Lupus La protein homolog	P32067	0.044	0.441	-2.266	6h + down vs 6h -
Protein disulfide-isomerase TMX3	Q8BXZ1	0.047	0.442	-2.264	6h + down vs 6h -
COMM domain-containing protein 7	Q8BG94	0.034	0.445	-2.249	6h + down vs 6h -
Torsin-1A-interacting protein 1	Q921T2	0.048	0.446	-2.243	6h + down vs 6h -
Proteasome adapter and scaffold protein ECM29	Q6PDI5	0.035	0.447	-2.239	6h + down vs 6h -
Programmed cell death 6-interacting protein	Q9WU78	0.019	0.447	-2.239	6h + down vs 6h -
26S proteasome non-ATPase regulatory subunit 12	Q9D8W5	0.035	0.447	-2.238	6h + down vs 6h -
Inter-alpha-trypsin inhibitor heavy chain H2	Q61703	0.017	0.448	-2.234	6h + down vs 6h -
Proteasome subunit alpha type-4	Q9R1P0	0.042	0.448	-2.231	6h + down vs 6h -
Lysine--tRNA ligase	Q99MN1	0.006	0.448	-2.231	6h + down vs 6h -
T-complex protein 1 subunit eta	P80313	0.014	0.449	-2.228	6h + down vs 6h -
Nuclear pore glycoprotein p62	Q63850	0.028	0.450	-2.223	6h + down vs 6h -
TAR DNA-binding protein 43	Q921F2	0.046	0.450	-2.222	6h + down vs 6h -
Methylosome protein 50	Q99J09	0.023	0.453	-2.208	6h + down vs 6h -
Calcium/calmodulin-dependent protein kinase type II subunit gamma	Q923T9	0.024	0.453	-2.207	6h + down vs 6h -
Talin-1	P26039	0.009	0.455	-2.197	6h + down vs 6h -
Heterogeneous nuclear ribonucleoprotein M	Q9D0E1	0.044	0.455	-2.196	6h + down vs 6h -
NHL repeat-containing protein 2	Q8BZW8	0.044	0.456	-2.191	6h + down vs 6h -
Vasodilator-stimulated phosphoprotein	P70460	0.045	0.457	-2.189	6h + down vs 6h -
[Pyruvate dehydrogenase (acetyl-transferring)] kinase isozyme 3, mitochondrial	Q922H2	0.034	0.459	-2.178	6h + down vs 6h -
Eukaryotic initiation factor 4A-II	P10630	0.019	0.469	-2.134	6h + down vs 6h -
Heterogeneous nuclear ribonucleoprotein F	Q9Z2X1	0.045	0.471	-2.122	6h + down vs 6h -
Brain-specific angiogenesis inhibitor 1-associated protein 2	Q8BKX1	0.016	0.474	-2.109	6h + down vs 6h -
Glutamine-rich protein 1	Q3UA37	0.002	0.474	-2.108	6h + down vs 6h -
N-terminal kinase-like protein	Q9EQC5	0.047	0.475	-2.105	6h + down vs 6h -
ATP-citrate synthase	Q91V92	0.042	0.476	-2.099	6h + down vs 6h -
Phosducin-like protein 3	Q8BVF2	0.039	0.478	-2.093	6h + down vs 6h -
Cytochrome b-c1 complex subunit Rieske, mitochondrial	Q9CR68	0.036	0.480	-2.085	6h + down vs 6h -
Ectonucleoside triphosphate diphosphohydrolase 5	Q9WUZ9	0.038	0.484	-2.068	6h + down vs 6h -
14-3-3 protein eta	P68510	0.039	0.484	-2.067	6h + down vs 6h -
60S ribosomal protein L8	P62918	0.008	0.485	-2.062	6h + down vs 6h -
AH receptor-interacting protein	O08915	0.023	0.487	-2.055	6h + down vs 6h -
Probable ATP-dependent RNA helicase DDX5	Q61656	0.036	0.487	-2.053	6h + down vs 6h -

Dymeclin	Q8CHY3	0.034	0.488	-2.049	6h + down vs 6h -
Zinc finger CCCH-type antiviral protein 1	Q3UPF5	0.036	0.488	-2.048	6h + down vs 6h -
Transformer-2 protein homolog beta	P62996	0.030	0.490	-2.040	6h + down vs 6h -
Lamina-associated polypeptide 2, isoforms alpha/zeta	Q61033	0.034	0.493	-2.028	6h + down vs 6h -
Mitotic checkpoint protein BUB3	Q9WVA3	0.036	0.494	-2.023	6h + down vs 6h -
Nodal modulator 1	Q6GQT9	0.006	0.495	-2.021	6h + down vs 6h -
Importin-5	Q8BKC5	0.039	0.495	-2.021	6h + down vs 6h -
Adenylate kinase 2, mitochondrial	Q9WTP6	0.021	0.496	-2.018	6h + down vs 6h -
2-oxoglutarate dehydrogenase, mitochondrial	Q60597	0.026	0.496	-2.014	6h + down vs 6h -
Vam6/Vps39-like protein	Q8R5L3	0.015	0.496	-2.014	6h + down vs 6h -
Exportin-2	Q9ERK4	0.015	0.500	-1.999	6h + down vs 6h -
Thimet oligopeptidase	Q8C1A5	0.026	0.501	-1.997	6h + down vs 6h -
Serine/threonine-protein phosphatase 6 catalytic subunit	Q9CQR6	0.010	0.501	-1.996	6h + down vs 6h -
Transportin-1	Q8BFY9	0.021	0.502	-1.992	6h + down vs 6h -
Fascin	Q61553	0.002	0.503	-1.988	6h + down vs 6h -
Protein PBDC1	Q9D0B6	0.003	0.503	-1.986	6h + down vs 6h -
SRA stem-loop-interacting RNA-binding protein, mitochondrial	Q9D8T7	0.045	0.504	-1.985	6h + down vs 6h -
Serine/threonine-protein kinase DCLK1	Q9JLM8	0.031	0.504	-1.985	6h + down vs 6h -
Hexokinase-2	O08528	0.005	0.504	-1.984	6h + down vs 6h -
14-3-3 protein theta	P68254	0.042	0.505	-1.979	6h + down vs 6h -
Pre-B-cell leukemia transcription factor-interacting protein 1	Q3TVI8	0.012	0.507	-1.972	6h + down vs 6h -
Nucleosome assembly protein 1-like 1	P28656	0.032	0.512	-1.954	6h + down vs 6h -
Protein-L-isoaspartate(D-aspartate) O-methyltransferase	P23506	0.017	0.514	-1.945	6h + down vs 6h -
Biliverdin reductase A	Q9CY64	0.030	0.517	-1.934	6h + down vs 6h -
Signal transducer and transcription activator 6	P52633	0.039	0.517	-1.933	6h + down vs 6h -
Eukaryotic translation initiation factor 3 subunit E	P60229	0.032	0.518	-1.929	6h + down vs 6h -
Dual specificity mitogen-activated protein kinase kinase 3	O09110	0.001	0.519	-1.928	6h + down vs 6h -
Mitochondrial import inner membrane translocase subunit TIM50	Q9D880	0.048	0.520	-1.925	6h + down vs 6h -
Protein PRRC1	Q3UPH1	0.039	0.520	-1.924	6h + down vs 6h -
Proteasome subunit beta type-7	P70195	0.017	0.522	-1.917	6h + down vs 6h -
40S ribosomal protein S20	P60867	0.042	0.524	-1.910	6h + down vs 6h -
Prefoldin subunit 2	O70591	0.036	0.524	-1.908	6h + down vs 6h -
Stress-70 protein, mitochondrial	P38647	0.013	0.525	-1.905	6h + down vs 6h -
ADP-ribosylation factor-like protein 3	Q9WUL7	0.033	0.527	-1.897	6h + down vs 6h -
Histidine--tRNA ligase, cytoplasmic	Q61035	0.048	0.532	-1.881	6h + down vs 6h -
von Willebrand factor A domain-containing protein 8	Q8CC88	0.004	0.536	-1.864	6h + down vs 6h -
Tyrosine-protein phosphatase non-receptor type 23	Q6PB44	0.029	0.537	-1.864	6h + down vs 6h -
4-aminobutyrate aminotransferase, mitochondrial	P61922	0.041	0.538	-1.859	6h + down vs 6h -
Enoyl-[acyl-carrier-protein] reductase, mitochondrial	Q9DCS3	0.007	0.539	-1.856	6h + down vs 6h -
Protein FAM98B	Q80VD1	0.020	0.539	-1.855	6h + down vs 6h -
116 kDa U5 small nuclear ribonucleoprotein component	O08810	0.012	0.540	-1.852	6h + down vs 6h -
26S proteasome non-ATPase regulatory subunit 6	Q99JI4	0.041	0.540	-1.851	6h + down vs 6h -
28S ribosomal protein S31, mitochondrial	Q61733	0.012	0.541	-1.848	6h + down vs 6h -
Glutamate dehydrogenase 1, mitochondrial	P26443	0.008	0.542	-1.845	6h + down vs 6h -
Dolichyl-diphosphooligosaccharide--protein glycosyltransferase subunit 2	Q9DBG6	0.018	0.542	-1.844	6h + down vs 6h -
Cytochrome b-c1 complex subunit 1, mitochondrial	Q9CZ13	0.027	0.543	-1.843	6h + down vs 6h -
Quinone oxidoreductase	P47199	0.040	0.544	-1.839	6h + down vs 6h -
Integrator complex subunit 4	Q8CIM8	0.044	0.546	-1.833	6h + down vs 6h -
Importin subunit beta-1	P70168	0.046	0.546	-1.831	6h + down vs 6h -
Histone H1.0	P10922	0.007	0.546	-1.830	6h + down vs 6h -
Conserved oligomeric Golgi complex subunit 1	Q9Z160	0.008	0.548	-1.825	6h + down vs 6h -
OCIA domain-containing protein 2	Q9D8W7	0.033	0.548	-1.823	6h + down vs 6h -
AMP deaminase 3	O08739	0.026	0.550	-1.819	6h + down vs 6h -
Heme-binding protein 1	Q9R257	0.006	0.552	-1.812	6h + down vs 6h -
Thioredoxin-like protein 1	Q8CDN6	0.026	0.554	-1.805	6h + down vs 6h -
Very long-chain specific acyl-CoA dehydrogenase, mitochondrial	P50544	0.041	0.555	-1.802	6h + down vs 6h -
Vigilin	Q8VDJ3	0.022	0.557	-1.794	6h + down vs 6h -
26S proteasome non-ATPase regulatory subunit 8	Q9CX56	0.043	0.558	-1.794	6h + down vs 6h -
Plexin-B2	B2RXS4	0.014	0.558	-1.792	6h + down vs 6h -
Protein unc-45 homolog A	Q99KD5	0.035	0.560	-1.786	6h + down vs 6h -

cAMP-dependent protein kinase type II-beta regulatory subunit	P31324	0.049	0.560	-1.784	6h + down vs 6h -
S-methyl-5'-thioadenosine phosphorylase	Q9CQ65	0.039	0.563	-1.778	6h + down vs 6h -
Eukaryotic translation initiation factor 3 subunit F	Q9DCH4	0.032	0.564	-1.775	6h + down vs 6h -
Periodic tryptophan protein 1 homolog	Q99LL5	0.005	0.568	-1.760	6h + down vs 6h -
THO complex subunit 4	O08583	0.034	0.569	-1.759	6h + down vs 6h -
WASH complex subunit 2	Q6PGL7	0.004	0.571	-1.751	6h + down vs 6h -
Staphylococcal nuclease domain-containing protein 1	Q78PY7	0.043	0.587	-1.704	6h + down vs 6h -
NPC intracellular cholesterol transporter 2	Q9Z0J0	0.027	0.587	-1.703	6h + down vs 6h -
Acid sphingomyelinase-like phosphodiesterase 3b	P58242	0.037	0.588	-1.702	6h + down vs 6h -
Guanine nucleotide-binding protein G(I)/G(S)/G(O) subunit gamma-5	Q80SZ7	0.044	0.589	-1.699	6h + down vs 6h -
Haloacid dehalogenase-like hydrolase domain-containing protein 2	Q3UGR5	0.019	0.589	-1.697	6h + down vs 6h -
Importin subunit alpha-5	Q60960	0.041	0.592	-1.690	6h + down vs 6h -
Cleft lip and palate transmembrane protein 1 homolog	Q8VBZ3	0.018	0.594	-1.684	6h + down vs 6h -
Eukaryotic translation initiation factor 3 subunit B	Q8JZQ9	0.046	0.598	-1.671	6h + down vs 6h -
Glutathione S-transferase A4	P24472	0.014	0.605	-1.653	6h + down vs 6h -
Transcription factor BTF3	Q64152	0.047	0.605	-1.653	6h + down vs 6h -
DNA mismatch repair protein Msh6	P54276	0.045	0.609	-1.642	6h + down vs 6h -
Dihydrofolate reductase	P00375	0.021	0.610	-1.639	6h + down vs 6h -
Peptidyl-prolyl cis-trans isomerase FKBP2	P45878	0.020	0.613	-1.630	6h + down vs 6h -
Coiled-coil domain-containing protein 102A	Q3TMW1	0.024	0.618	-1.619	6h + down vs 6h -
39S ribosomal protein L13, mitochondrial	Q9D1P0	0.009	0.624	-1.602	6h + down vs 6h -
UHRF1-binding protein 1-like	A2RSJ4	0.050	0.625	-1.601	6h + down vs 6h -
CCR4-NOT transcription complex subunit 11	Q9CWN7	0.050	0.630	-1.587	6h + down vs 6h -
Mitochondrial import inner membrane translocase subunit TIM44	O35857	0.034	0.649	-1.541	6h + down vs 6h -
Dynein assembly factor 5, axonemal	B9EJR8	0.048	0.653	-1.531	6h + down vs 6h -
Alpha-1,3/1,6-mannosyltransferase ALG2	Q9DBE8	0.040	0.655	-1.527	6h + down vs 6h -
2-amino-3-ketobutyrate coenzyme A ligase, mitochondrial	O88986	0.041	0.663	-1.508	6h + down vs 6h -
Biogenesis of lysosome-related organelles complex 1 subunit 4	Q8VED2	0.043	0.671	-1.490	6h + down vs 6h -
DDRGK domain-containing protein 1	Q80WW9	0.011	0.671	-1.490	6h + down vs 6h -
CTP synthase 1	P70698	0.044	0.674	-1.483	6h + down vs 6h -
Heterogeneous nuclear ribonucleoprotein H2	P70333	0.000	0.684	-1.462	6h + down vs 6h -
Methylthioribulose-1-phosphate dehydratase	Q9WVQ5	0.011	0.691	-1.446	6h + down vs 6h -
39S ribosomal protein L39, mitochondrial	Q9JKF7	0.014	0.698	-1.432	6h + down vs 6h -
Peroxisomal membrane protein PMP34	O70579	0.043	0.701	-1.427	6h + down vs 6h -
Pyroglutamyl-peptidase 1	Q9ESW8	0.032	0.702	-1.424	6h + down vs 6h -
Actin-related protein 2/3 complex subunit 5	Q9CPW4	0.015	0.734	-1.363	6h + down vs 6h -
Nucleolysin TIAR	P70318	0.035	0.752	-1.330	6h + down vs 6h -
Peroxisomal acyl-coenzyme A oxidase 3	Q9EPL9	0.007	0.767	-1.304	6h + down vs 6h -
Alpha-2-macroglobulin receptor-associated protein	P55302	0.039	0.768	-1.302	6h + down vs 6h -
Anaphase-promoting complex subunit 13	Q8R034	0.012	0.777	-1.287	6h + down vs 6h -
NFU1 iron-sulfur cluster scaffold homolog, mitochondrial	Q9QZ23	0.032	0.778	-1.285	6h + down vs 6h -
Serine/threonine-protein kinase 24	Q99KH8	0.038	0.797	-1.254	6h + down vs 6h -
U5 small nuclear ribonucleoprotein 40 kDa protein	Q6PE01	0.010	0.806	-1.241	6h + down vs 6h -
Putative hydroxypyruvate isomerase	Q8R1F5	0.047	1.188	1.188	6h + up vs 6h -
Protein LSM12 homolog	Q9D0R8	0.006	1.312	1.312	6h + up vs 6h -
Vesicle-associated membrane protein 7	P70280	0.041	1.318	1.318	6h + up vs 6h -
Mixed lineage kinase domain-like protein	Q9D2Y4	0.029	1.359	1.359	6h + up vs 6h -
Methionine adenosyltransferase 2 subunit beta	Q99LB6	0.022	1.377	1.377	6h + up vs 6h -
Peroxisomal membrane protein PEX14	Q9R0A0	0.021	1.444	1.444	6h + up vs 6h -
Protein mono-ADP-ribosyltransferase PARP4	E9PYK3	0.043	1.472	1.472	6h + up vs 6h -
Sorbin and SH3 domain-containing protein 1	Q62417	0.042	1.534	1.534	6h + up vs 6h -
Protein ABHD16A	Q9Z1Q2	0.039	1.566	1.566	6h + up vs 6h -
Cytochrome c oxidase subunit 7A2, mitochondrial	P48771	0.022	1.584	1.584	6h + up vs 6h -
Core histone macro-H2A.1	Q9QZQ8	0.031	1.585	1.585	6h + up vs 6h -
U6 snRNA-associated Sm-like protein LSm1	Q8VC85	0.043	1.589	1.589	6h + up vs 6h -
Protein FAM98A	Q3TJZ6	0.010	1.703	1.703	6h + up vs 6h -
Ras-related protein Rab-10	P61027	0.048	1.791	1.791	6h + up vs 6h -
N-acetylgalactosamine kinase	Q68FH4	0.031	1.835	1.835	6h + up vs 6h -
Uracil phosphoribosyltransferase homolog	B1AVZ0	0.014	2.071	2.071	6h + up vs 6h -
Cadherin-11	P55288	0.014	2.173	2.173	6h + up vs 6h -
ATPase family AAA domain-containing protein 3	Q925I1	0.033	2.258	2.258	6h + up vs 6h -
CREB-regulated transcription coactivator 1	Q68ED7	0.032	2.322	2.322	6h + up vs 6h -

Huntingtin	P42859	0.018	2.447	2.447	6h + up vs 6h -
Proteolipid protein 2	Q9R1Q7	0.049	2.500	2.500	6h + up vs 6h -
F-box-like/WD repeat-containing protein TBL1XR1	Q8BHJ5	0.036	2.513	2.513	6h + up vs 6h -
Erlin-1	Q91X78	0.046	2.532	2.532	6h + up vs 6h -
ATP synthase subunit g, mitochondrial	Q9CPQ8	0.050	2.817	2.817	6h + up vs 6h -
Growth arrest-specific protein 1	Q01721	0.014	3.677	3.677	6h + up vs 6h -
NADH dehydrogenase [ubiquinone] 1 beta subcomplex subunit 9	Q9CQJ8	0.009	4.858	4.858	6h + up vs 6h -